An Assessment of Predictive Models for Operational Management of a Reservoir in a Data-Scarce Basin:
A Case Study of the Black Volta Basin

Master thesis

M.B.L.M. Kasteel

August 2023

Delft University of Technology

Master thesis

An Assessment of Predictive Models for Operational Management of a Reservoir in a Data-Scarce Basin: A Case Study of the Black Volta Basin

by
M.B.L.M. Kasteel

August 2023

A master thesis submitted to the Delft University of Technology in partial fulfillment for the degree of
Master of Science
in Civil Engineering specialized in Water Management.

Defense:	August 1st 2023
Student number:	4884671
Thesis committee:	Prof. dr. ir. N.C. van de Giesen
	Dr. ir. E. Abraham
	Dr. M. Hrachowitz

TEMBO Africa: *The work leading to these results has received funding from the European Horizon Europe Programme (2021-2027) under grant agreement n° 101086209. The opinions expressed in the document are of the authors only and no way reflect the European Commission's opinions. The European Union is not liable for any use that may be made of the information.*

Preface

"Discharge Simulation in a Data-Scarce Basin: A Case Study of the Black Volta Basin". This is the work of one civil engineering master student in Water Management at Delft University of Technology. This work has been made in collaboration with the Bui Power Authority and TEMBO Africa.

I would like to express my sincere gratitude to my supervisor, Prof.dr.ir. Nick van de Giesen, for enabling my involvement in this project and providing invaluable guidance and advice throughout its duration. Additionally, I extend my appreciation to Dr.ir. Edo Abraham for his valuable support and contributions to the project. Furthermore, I am thankful to my last supervisor, Dr. Markus Hrachowitz, for his expert guidance in developing the hydrological model and for offering highly valuable feedback.

I want to extend my heartfelt appreciation to Ir. Abraham Baffoe-Sersah ("AB") for his exceptional hospitality during my time in Bui. AB's support and guidance were invaluable during my stay, and I am truly grateful for his assistance. I would also like to express my gratitude to Philip Ato Ankoh and all the employees of BPA for their remarkable assistance and willingness to help.

Moreover, I want to acknowledge and express my gratitude to my great friend and travel companion (soon to be "Ir") Niels Hoogendoorn. Our shared journey to Ghana was an unforgettable experience, combining work and student life, and creating lifelong memories.

Additionally, I would like to thank the Trans-African Hydro-Meteorological Observatory (TAHMO) for providing the meteorological data used in this project. Interested parties can contact info@tahmo.org for access to this data.

Last, but not least, I am deeply grateful to the funding provided by various sources, namely the Lamminga Fund, FAST TU Delft ("Funding Ambitious STudents"), and Delft Global Initiative. The generosity of these funds made my trip to Ghana possible, and I am sincerely thankful for their support.

Abstract

The Bui Dam, the second-largest hydropower dam in Ghana, plays a significant role in the sustainable energy mix of the country. It is managed by the Bui Power Authority (BPA) and has a capacity of hydro-clean generation of 404MW, contributing to 17% of the country's total electricity generation. However, decision-making at the dam lacks the use of predictive models and meteorological measurements. This can lead, in the case of perceived flooding risks and high dam water levels, to valuable water being spilled and endangering the downstream areas. Balancing the tradeoff between energy production and safety can be effectively achieved by implementing predictive models that anticipate peak flows in advance.

Since its commissioning in 2013, the Bui Dam has experienced two instances of emergency spillage, resulting in significant financial losses, property destruction, and displacement of downstream communities. Currently, the reservoir management decision-making process uses two discharge stations upstream, with one of them yielding some unreliable outcomes for high flows. Therefore, it is crucial to prioritize the analysis and updating of rating curves to ensure accurate forecasting.

This research aims to address these limitations by recalibrating the rating curve using the reservoir balance in a conservative manner, i.e. leaning on the safe side to avoid overestimation. Additionally, a conceptual, semi-distributed model was developed simulating high flows, specifically focusing on the years 2019 and 2022 when spillage events occurred. Five different hydrological conceptual models, with three different structures: single, serial, and parallel structures, were tested. The serial model yielded the best results. Then the Black Volta Basin was divided into five sub-catchments, and each sub-catchment was lumped. In the absence of discharge data for the upstream sub-catchments, remote sensing data from GRACE and satellite altimetry (3 virtual stations with data from 2016 to 2022) were used to impose restrictions on the feasible model parameter sets, thereby improving accuracy.

The final model output was calibrated using discharge data obtained from the recalibrated rating curve, along with satellite altimetry data. In the calibrated benchmark case, the model effectively reproduced daily river flows, demonstrating an optimum Nash-Sutcliffe efficiency (NSE) of 0.85 for the period of 2018 to 2022.
Subsequently, the model underwent extensive testing under various conditions, including an independent time period without recalibration, different precipitation input sources, transitioning from actual evapotranspiration (AET) to potential evapotranspiration (PET) input, and a change in the testing discharge location. Throughout these testing phases, the model consistently produced favorable results, with NSE values ranging from 0.74 to 0.86.

Furthermore, the model was tested for its progressive predictive capability in simulating the unexpected peak inflows that led to the spillage event in 2019, utilizing

only precipitation data from the TAHMO precipitation stations, which are openly accessible with near-live timing. The model successfully predicted the occurrence of the large peak inflow, on October 22nd, which ultimately caused the spillage. The model anticipated the occurrence of the ”unexpected” second peak, to some extent, as early as October 12th, providing an 11-day predicting window.

Overall, this research enhances the understanding of the Bui Dam system by implementing a recalibrated rating curve and developing a conceptual model that incorporates remote sensing data. The results demonstrate the model's capability to simulate past events accurately and predict future inflow patterns, thereby providing valuable insights for effective dam management and spillage prevention.

One significant discovery regarding the character of the Black Volta River at the Bui Dam is the limitation of the prediction period to a strict maximum of two weeks. While the model proves effective within this time-frame, it is advisable for future research to consider incorporating weather predictions to extend this window further. Doing so would enhance the model's forecasting capabilities and provide even more valuable information for dam operators and decision-makers.

Contents

List of Figures

1 Introduction

1.1 Background

The Black Volta River, originating from Burkina Faso, flows into the Volta Lake formed by the Akasombo dam. It has a mean annual runoff of 7673x10^{6}m^3 or 243 m^3/s, representing 18% of the total runoff in the Volta Lake [Andreini et al., 2000]. The Black Volta River has significant potential for generating sustainable and reliable electricity, particularly for the northern region of Ghana. To harness this potential, the government of Ghana initiated the construction of the Bui Dam in 2009. Located at the boundary between the Savannah and Bono regions, the Bui Dam was commissioned in December 2013 and is managed by the Bui Power Authority (BPA). It has an installed capacity of 404MW, consisting of four generating units, including three 133.33MW Francis Turbine Units and a 4MW Turbinette. The dam is a concrete gravity dam with a maximum height of 108m and a crest length of 492.5m.
Additionally in 2019, with the aim of increasing renewable energy in the country's energy mix by 10%, a 250MW solar project was started. The first 50MW solar PV was installed in November 2020. Currently, BPA also studies and tests the possibility of installing floating solar on the Bui reservoir.

BPA has a mandate to plan, execute and manage the Bui Hydroelectric project. It makes sure that the dam is working in a safe and reliable way and is ready to generate at all times. However, BPA is not in control of when and how much electricity is going to be generated. Managing the national electricity grid is a very complicated task of matching the electricity demand and offer at any given time. This task is managed by the company GridCo. Every morning BPA measures the reservoir water level and communicates to GridCo a range of how much electricity can be generated during that day. GridCo then processes that information along with all the other electricity generation plants across the country and orders BPA to generate a specific amount of electricity during the day. Usually, that demand fluctuates over the day.
The main conclusion about this process is that BPA does not have control on how much electricity they are going to generate. Except when the dam reaches critical levels, they have the possibility to request to GridCo to produce more or less electricity.

1.2 Problem analysis

On the 23rd of October 2019, the Bui Power Authority made a controlled spillage, releasing a total of 538 Mm^3, resulting in substantial financial losses of unproduced electricity, the destruction of properties, and thousands of people displaced downstream of the dam. The spillage was necessary because the dam was reaching dangerous maximal water levels due to an unlikely wet October month. Again, three years later on the 12th of October 2022, BPA used the emergency spillway. This time however in the context of a precautionary safety test. However the year 2022 was the year with the highest discharge recorded in the past 30 years and the dam was again reaching maximal levels, so it is unclear if even without the safety exercise, a spillway would have been necessary.

BPA's primary objective during each rainy season is to maximize the reservoir's water storage capacity by filling it to the highest possible level. This approach aims to ensure an ample water supply throughout the subsequent dry season. At the moment, the main strategy behind the dam operations of BPA is to work in a risk-averse manner. BPA prefers to steer clear of the repercussions of inaccurate forecasts at the expense of unrealized benefits, consequently, it is difficult to accommodate for unexpected large discharge increases as in 2019. Nevertheless, multiple studies using different forecasting methods all praised the benefits of combining forecasts with hydropower generation [Hamlet et al., 2002] [Block, 2011] [Lima and Lall, 2010].

In the Volta Basin, the temporal variability of runoff is characterized by a greater magnitude compared to the substantial year-to-year fluctuations in precipitation. Research conducted by Andreini et al. [2000] reveals that while the mean coefficient of variation for rainfall in the Volta Basin stands at 7%, it significantly escalates to 57% for river discharge. This notable disparity emphasizes the heightened sensitivity of runoff to variations in rainfall. Consequently, even minor changes in annual precipitation can lead to significant modifications in river flow [Obeng-Asiedu, 2004]. This variability underscores the need for a robust hydrological model that can accurately identify the specific changes in precipitation capable of causing significant modifications in discharge.

A study from Jin et al. [2018] applied high climate forcing scenario RCP8.5 to the Volta river system and showed that during the rainy season, the extreme high flows (Q5) of the Black Volta River are projected to increase by 11% in 2050 and by 36% in 2090 Jin et al. [2018]. This again shows the necessity of implementing an hydrological model to better accommodate this increase and avoid spillage like on the 23rd of October 2022. Implementing effective forecasts results in an increase in electricity generation, and fewer spills while the reliability of storage reservoir refill remains mainly unaffected. Additionally, combining forecast methods with electricity production is particularly impactful and efficient when there is a high likelihood of larger streamflows Hamlet et al. [2002].

At present, the only information that BPA uses to make decisions about the future is daily discharge measurements in Chache and Lawra, respectively 105 km and 320 km from the reservoir, giving them a 1 to 3-day range inflow forecast window. Further, BPA does not utilize hydrological models or forecasting methods; however, there is a keen interest in incorporating them into their operations. To achieve this goal, BPA is collaborating with TEMBO Africa ('Transformative Environmental Monitoring to Boost Observations'), which provides cost-effective innovative sensors and reservoir management services. The aim of this collaboration is to enhance BPA's capabilities in its decision-making process.

1.3 Research question

This report serves as preliminary research, focusing on studying the hydrological footprint of the Black Volta Basin and exploring the potential benefits and limitations of hydrological modeling in enhancing reservoir management. The main goal of the study is to make a hydrological model on a daily temporal scale that can correctly model the discharges that caused spills in 2019 and 2022. However, because the spill in 2022 was a safety exercise, the testing will focus more on the one in 2019. Ideally, the hydrological model should be able to function using only TAHMO stations. In this context, it is important to understand the different rainfall distributions and catchment characteristics. The main research question of this thesis is:

"How can the daily discharge be effectively modeled in the data-scarce Black Volta Basin?".

The main research question will be answered based on the answers from the following sub-questions:

-*"Which datasets are available and reliable enough to be used to calibrate and test the hydrological model"*

-*"What is the impact of the different sub-catchments on the total discharge of the Black Volta"*

-*"Could the spills of 2019 be avoided using a hydrological model and TAHMO precipitation inputs"*

1.4 Structure

Chapter 2 "Study Site and Data" focuses on the comprehensive examination of the Black Volta basin, which encompasses five sub-catchments. This chapter ensures the consistency and accuracy of all the data used in the hydrological model.

In Chapter 3 "Methodology" the chapter is divided into two parts. The first part provides a detailed explanation of the methodology employed to update the Chache rating curve. The second part describes the entire process of developing, calibrating, and testing the hydrological model.

Moving on to Chapter 4 "Results and Discussion" it presents the newly established rating curve for Chache and discusses its reliability. Furthermore, this chapter presents the results obtained from the hydrological model.

Finally, Chapter 5 "Conclusion" concludes the study by summarizing the findings and offering recommendations for further research in the field.

2 Study area and data

2.1 Study area

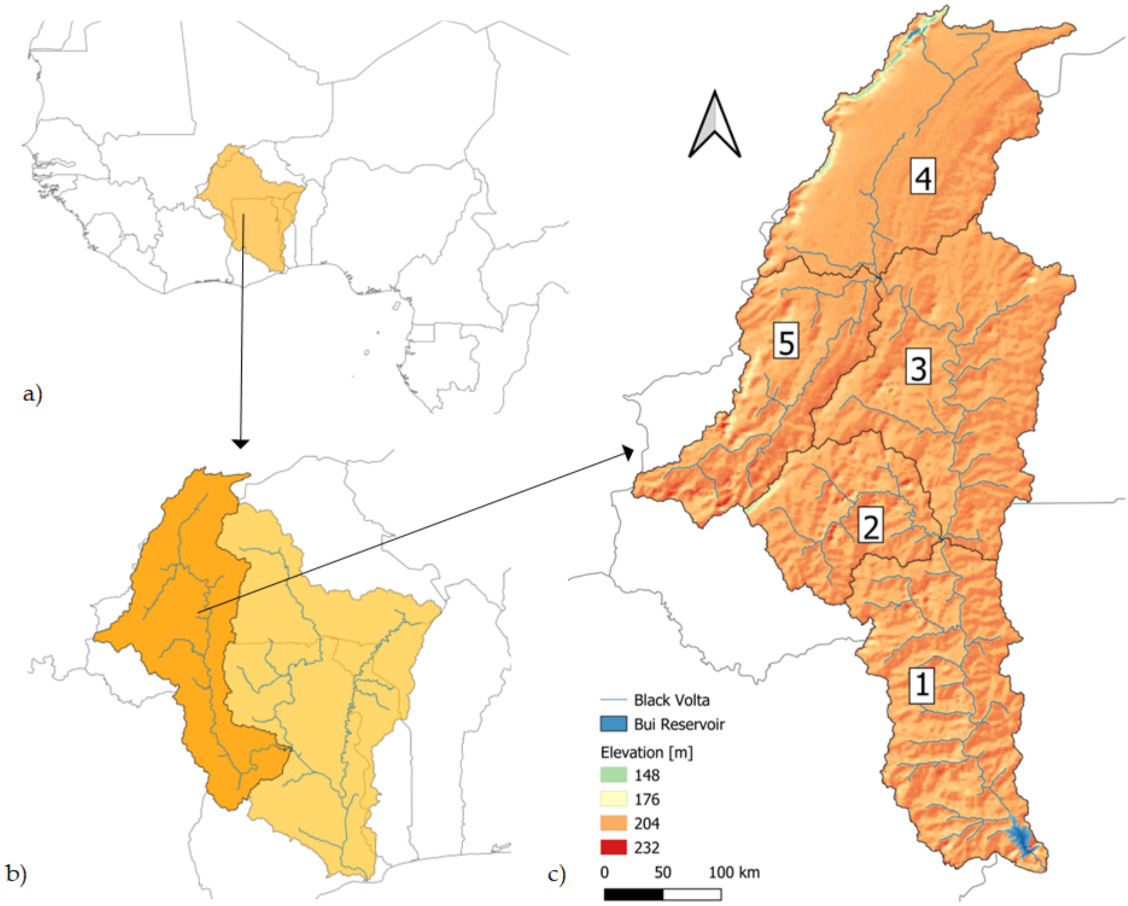

Figure 2.1: a) Map of the whole Volta Basin, a transboundary basin shared by six riparian countries b) Black Volta Basin accounting for 18% of total runoff in the Volta Lake c) DEM of the Black Volta Basin (BVB), which, in the context of this research, has been reduced such that the Bui reservoir is the most downstream part of the basin. The BVB was then divided into 5 sub-catchments based on the Strahler order

The study focuses on the Black Volta basin, which spans between Latitude 7°00100″ N and 14°30100″ N and Longitude 5°30100″ W and 1°30100″ W. It covers an estimated area of approximately 131,104 km2 (with the Bui reservoir being the downstream boundary) and is a transboundary river system that extends across Mali, Burkina Faso, Ghana, and Cote d'Ivoire. In 2000, the basin had a population of around 4.5 million people which is expected to grow to 8 million people by the 2025 [Consult, 2012], with varying population densities ranging from 8 to 133 people/km^2. The Lawra district in Ghana has the highest population density within the basin.

For the purpose of this research, the Black Volta basin was partitioned into five catchments based on the Strahler order level 5 [Strahler, 1957], see Figure 2.1.c. The decision to divide the catchment at this specific order level was primarily driven by data availability (or scarcity). Among the catchments, sub-catchment 5 represents the most upstream portion, while sub-catchment 1 is the most downstream sub-catchment. Sub-catchment 1 was modified to account in such a way that the Bui Dam is situated at the downstream end of the entire catchment. In this research, for the sake of convenience, the term "catchment" will be used instead of "sub-catchment."

The vegetation zones within the study site exhibit a north-to-south orientation. Starting from the sparsely vegetated Sahel in the north, the vegetation transitions through savannah regions and finally culminates in the Guinea forest zone or rainforest in the extreme south.

The climate of the study site is characterized by a distinct dry and wet rainfall pattern. The majority of the annual rainfall, over 70%, occurs during the months of August, September, and October. In contrast, the months of November to March experience minimal to no rainfall in most parts of the basin.

The geology of the Black Volta Basin predominantly consists of granitoid. The basin is underlain by crystalline basement complex rocks and well-consolidated sedimentary formations that share similar characteristics to the crystalline basement complex rocks. These rocks are primarily impermeable and lack primary porosity. However, secondary porosities develop through processes such as jointing, fracturing, faulting, or weathering. The weathered zone serves as a reservoir for groundwater storage, and the occurrence of groundwater in the Black Volta Basin is mainly influenced by the development of these secondary porosities [Jung, 2006].

Catchment 5

The Black Volta River, known as the Mouhoun in the Burkinabe area, originates from its headwater source in the Banfora Cliffs near the town of Bobo-Dioulasso. Unlike other rivers in the basin, where most of them run dry during the dry season, the Mouhoun remains the only permanent river [Jung, 2006]. As it enters Catchment 5, it flows in a northeastward direction. This catchment extends until it receives a Sahelian stream from catchment 4 on its left bank, providing the main river with a limited water supply. According to the FAO Land Cover Classification, the primary soil type in catchment 5 is Rainfed Cropland [FAO, 1998]. The size of Catchment 5 is 20.4 *10^3 km^3, representing 17.1% of the total catchment (but the total catchment again reduced such that this time Chache, a discharge station important for the hydrological model, being the downstream boundary).

Catchment 4

The river that originates from Mali in catchment 4 and joins the Mouhoun is called the Sourou, and during the wettest months of the rainy season, a relatively rare process is occurring. The Sourou River flows through a geographical depression known as the Sourou Depression. During the rainy season, when the Mouhoun's discharge surpasses a certain level, water from the river diverts into the Sourou Depression, where it is stored. In times of low flow, the stored water is released back into the Mouhoun, helping to manage the flood wave [Shahin, 2003] [Jung, 2006]. The Sourou depression actually acts as a natural regulator of Mouhoun's water runoff. In 1984, an additional regulation mechanism was implemented to control the flow of water and enable storage of up to 250*$10^6$$m^3$ of floodwater, subsequently releasing some of the surplus water back into the Mouhoun during the dry season [Bro, 2001]. And from the research of Shahin [2003], it was determined that downstream of the Sourou, specifically at the Boromo gauge station, the Mouhoun (Black Volta) exhibits a remarkably low yearly runoff coefficient of less than 3%, attributed to the presence of the depression and the flatness of the terrain, see Figure 2.2. The primary soil type in Catchment 4 is Rainfed Cropland and Grassland. The size of the catchment 4 is 31.1*10^3 km^3, representing 25.9% of the total catchment.

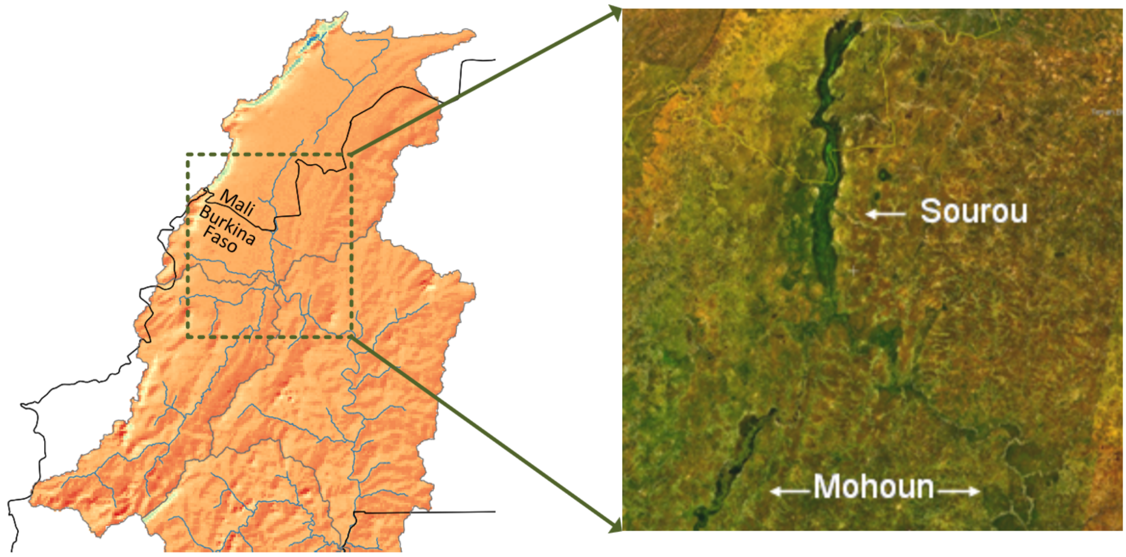

Figure 2.2: Left: Zoom in of DEM of the Black Volta Basin (BVB), it can be observed that the north of the catchment is a predominantly flat area, Right: Sourou Depression (source: [Jung, 2006]

Catchement 3, 2 and 1

As the Black Volta River flows southward, it merges with a series of small streams that exhibit a transient-tropical regime. The precipitation and the runoff fraction of precipitation gradually increase from north to south along its course. In Catchment 3, the average yearly precipitation is ranging from 890mm to 1050mm in Catchment 1. Additionally, the soil type undergoes a transition from Cropland Rainfed in the north to Shrubland and eventually to a closed, mixed type of Tree cover as we move south (FAO, 1998).

Moving downstream from the point where catchments 2 and 3 intersect, the first daily discharge station, Lawra, is located. BPA has been collecting daily discharge data in Lawra for the past 20 years, albeit with some gaps in certain years. Roughly 220 km further down the river, the second daily discharge station is found called Chache, which has a data collection record spanning 25 years. More detailed information about these discharge measurements will be provided in the upcoming Sections. The size of catchment 3, 2, and 1 is respectively $34.5*10^3$ km^3, $15.2*10^3$ km^3 and $18.6*10^3$ km^3, representing 28.7%, 12.7% and 15.6% of the total catchment (with Chache being the downstream boundary).

2.2 Data

One of the research project's main challenges was finding reliable, daily historical and actual data in the data-scarce Black Volta region. A lot of time and effort was put into selecting, acquiring, and checking the following data sources. In Figure 2.3, an overview was made with all the different rain and discharge gauges.

2.2.1 Precipitation

TAHMO

The Trans-African Hydro-Meteorological Observatory (TAHMO) aims to develop a vast network of weather stations across Africa openly accessible for scientific research and governmental applications. In the Black Volta basin, the first stations were installed in 2017, and currently over 16 stations are installed and this number is likely to increase in the future. As it can be seen in Figure 2.4, an installed station does not mean that it is operational all the time. This can be explained due to different reasons like empty batteries, faulty sensors, broken stations due to storms,...

One of the biggest advantages of the TAHMO stations compared to all the other precipitation sources is that the measured data is easily and almost immediately accessible (a couple of hours delay) after the rain event. This accessibility over the whole Black Volta basin is of crucial importance for predicting the inflows in the reservoir. The final aim of the research is to use TAHMO data in the hydrological model as only precipitation input.

The double mass curve method [Searcy and Hardison, 1960] was employed to analyze and check the in situ rainfall data. The method serves to assess the consistency of rainfall data by comparing the data from a single station with that of a composite pattern encompassing several other stations within a similar study area climate. If the plotted points on the double mass curve exhibited a close fit along a straight line, it indicates reliable data. By applying this method a couple of precipitation years from different stations were discarded.

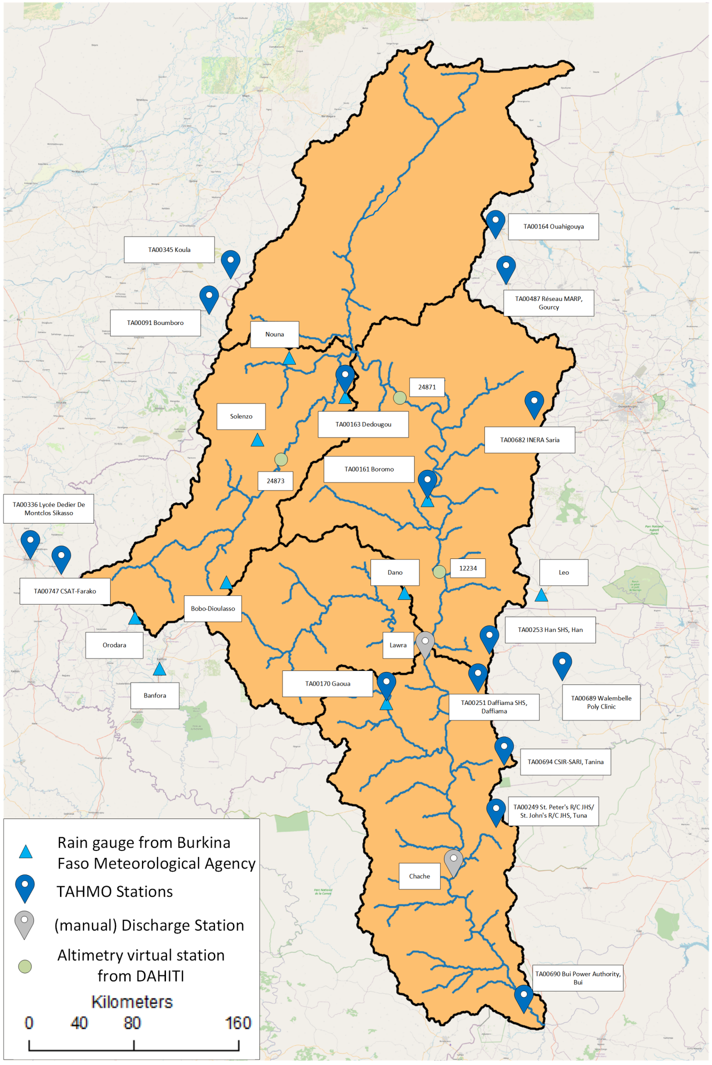

Figure 2.3: Black Volta basin stations overview. There are four different information sources: first the rain gauges from the Meteorological Agency of Burkina Faso (blue triangles). Next all the installed (but not all operational) TAHMO stations (blue pinpoints). Then there is the two manual discharge stations Chache and Lwara (grey pinpoint). Lastly the three altimetry stations from DAHITI (green circle)

Direction Générale de la Météorologie du Burkina Faso

The meteorological agency of Burkina Faso has shared its daily precipitation data for 11 of its stations in the Black Volta basin from 1991 to 2022. These stations are located in Banfora, Bobo-Dioulasso, Boromo, Dano, Dédougou, Gaoua, Léo, Nouna, Orodara, and Solenzo, see Figure 2.3. The data was again checked with the double mass curve, and every station except Leo, which needed some corrections, exhibited a straight line indicating consistent data. This data is of great importance for the calibration and testing of the hydrological model. In Gaoua, Boromo, and Dédougou, there are weather stations operated by TAHMO as well as stations managed by the meteorological agency of Burkina Faso. These three locations provide an excellent opportunity to compare data from the two sources. The precipitation measurements obtained from these stations exhibited a high degree of similarity, indicating a reliable

	2017	2018	2019	2020	2021	2022
TA00690						
TA00249					not Aug	
TA00694					half	half
TA00251						
TA00170		not Oct				
TA00689						
TA00253						
TA00161						
TA00682					not Sept	
TA00163						
TA00747					not Sept	
TA00336						
TA00091						
TA00345						
TA00487					not until June	
TA00164						

Figure 2.4: Overview availability TAHMO stations: some stations have missing months or the first part of the wet season. The data in this table was checked and classified as reliable

and consistent data source for both origins. Note that the precipitation registration data of the meteorological agency of Burkina Faso throughout the day does not follow the midnight-to-midnight pattern seen in the TAHMO data. Instead, it begins at 6 AM. Thus a two-hour-long precipitation event from 5 AM to 7 AM means that it will be divided over the day before and the day itself.

National Centers for Environmental Information

The National Centers for Environmental Information (NCEI) gives open access to a lot of environmental data around the world [Menne et al., 2012]. In the Black Volta basin, 7 stations are available with daily precipitation data ranging from 1973 to 2022. The stations are located Wa, Bole, Gaoua, Bobo-Dioulasso, Ouahigouya, Boromo, and Bondoukou. The data was again checked with the double mass curve and the results were not good. Also, the stations in Bobo-Dioulasso, Gaoua, and Boromo were compared with the ones from the meteorological agency of Burkina Faso above. The data from NCEI showed a lot of gaps, lasting from a couple of days to sometimes a couple of months. The yearly sums for all the stations were consistently largely underestimating the precipitation data of the Burkina Faso meteorological agency. For these reasons, it was decided to not use any data coming from the NCEI source.

Satellite precipitation products

A lot of different satellite products give access to daily historical precipitation data in the Black Volta Basin. However different papers [Logah et al., 2021], [Dembélé and Zwart, 2016], [Satgé et al., 2020] do not recommend the use of satellite products in the basin at a daily temporal scale because of its poor performance and reliability about the character and intensity of the daily precipitation. However, at a monthly scale, from the above-mentioned papers, the CHIRPS is the most recommended satellite product in the area [Funk et al., 2014].

Interpolation

Due to the availability of a long, consistent, and reliable precipitation dataset obtained from the meteorological agency of Burkina Faso, this dataset was selected for the purpose of calibrating and partially testing the hydrological model. The presence of spatial heterogeneity in system drivers, such as rainfall patterns, should not be overlooked. Attempting to average out this heterogeneity and its extreme values in threshold processes would result in a misrepresented understanding of the system's response. This is because threshold processes are heavily influenced by these extreme values. The Thiessen polygons interpolation method [Thiessen, 1911] is best suited to interpolate against that and was employed with an adequate number of stations in catchments 2, 3, and 5.

However, for catchments 1 and 4, there is only a single station available. Notably, in Catchment 4 ('Nouna'), the station is situated south of Catchment 4, resulting in a significant reduction in precipitation as one moves towards the northern part of the catchment. Conversely, for catchment 1, the only available station (known as 'Gaoua') is located in the northern part of the catchment. The decentralized placement of precipitation stations in these catchments makes it impractical to interpolate the data across the entire area of catchments 1 and 4.

To address this limitation, precipitation data from the Climate Hazards Group InfraRed Precipitation with Station data (CHIRPS) was utilized. To maintain some degree of consistency in data sources during the hydrological modeling, the following procedure was implemented: the CHIRPS precipitation data for the whole area of catchments 1 and 4, as well as the data from the individual points Gaoua and Nouna, were downloaded. A comparison was made between the point-scale and area-scale data, and the discrepancy factor between the point- and area-scale was determined for each month of each catchment. Subsequently, this factor was applied to the data obtained from the stations of the Burkina Faso Meteorological Agency and was used for the modeling.

2.2.2 River discharges

Discharges from Bui Power Authority

Since studying the possibility of building the Bui reservoir, the Bui Power Authority keeps track of the daily discharges in Chache and Lawra (see Figure 2.3). Every day during the dry season and twice a day during the wet season the water level is measured. Then using a rating curve the river discharge is calculated. This has been done in Chache from 2000 to the present (missing 2011 and 2012 due to the construction of the dam) and in Lawra from 2010 to the present (but only 7 years have usable years for hydrological modeling i.e. no significant gaps). The flow distance between Chache and Lawra is 218km and there are no major tributaries flowing into the Black Volta between these two stations. The unprocessed data can be seen in Figure 2.5

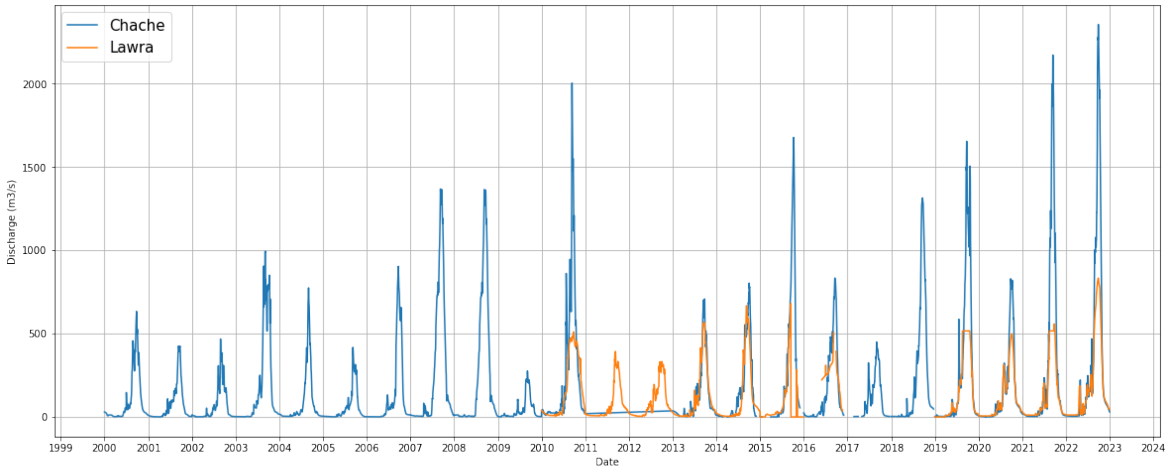

Figure 2.5: Discharge measured by BPA for station Chache and Lawra

Upon analyzing and comparing the data from the Chache and Lawra discharge stations, it becomes apparent that the discharge at Chache can exceed Lawra's measurements by more than 2.5 times. Given the absence of major tributaries between these two stations, such a significant disparity suggests the presence of an anomaly. Consequently, a field trip was conducted to investigate the measurement location at Chache and seek an explanation for this substantial difference.

Giving some context: during the wet season, the water flows over the floodplains, resulting in a maximal additional width of over 500 meters on each side (bearing in mind that the normal width of the Black Volta is 120 meters under regular flow conditions!). The rating curve currently in use was established based on river water levels below 4.6 meters when the flow was contained within the riverbanks. This rating curve was then extrapolated to cover higher water levels above the river banks. However, it overlooks important factors introduced by the floodplains, such as the presence of trees, bushes, and rocks, which significantly affect the friction coefficient.

The use of a constant friction coefficient in discharge calculations leads to an overestimation of discharge values when water levels exceed the river banks (above 4.6 meters). Consequently, there is a need to recalibrate the rating curve to address this issue before it can be effectively applied to calibrate and test the hydrological model. The upcoming chapter (Chapter 3.1) focuses on the necessary recalibrating of the rating curve to improve accuracy in these calculations.

Discharges from Global Runoff Data Centre

The primary objective of the Global Runoff Data Centre (GRDC) [Centre, 2019] is to enable research on worldwide climate patterns by providing access to environmental impacts and risks through the storage of data, and promoting long-term hydrological studies on a global scale. The GRDC is responsible for maintaining quality-controlled historical data on mean daily and monthly discharge. In the Black Volta, the GRDC has records of daily discharges in Lawra from 1975 to 2007. However, only 8 years (1991 to 1996, 1998, 2002, 2004, and 2005) do not have any gaps and can be used for the model.

2.2.3 Evapotranspiration

Potential

Potential evapotranspiration data in the basin is extracted from the Moderate Resolution Imaging Spectroradiometer (MODIS) instrument on the NASA Terra Platform satellite launched in 1999. This instrument measures the leaf area index, land cover type, and albedo at an 8-day temporal scale and 0.5 km spatial resolution. It takes daily meteorological inputs such as global daily temperature, actual vapor pressure, and incoming solar radiation. Then the MOD16 algorithm uses the Penman-Monteith equation [Mu et al., 2011] to calculate the potential evapotranspiration.

Actual

The MOD16 product, adding a surface conductance model, also calculates the actual evapotranspiration. However, when checking this evapotranspiration data into the water balance over the catchment results in a large inequality. It can be seen that the actual evapotranspiration from MOD16 underestimates the actual evapotranspiration from the water balance by a factor of approximately 2.5 over the long-term water balance. This is why the MOD16 Ea will not be used any further in the study.

Nevertheless, the paper Weerasinghe et al. [2020] compares nine different remote-sensing actual evapotranspiration products. From this paper, for the region of the Black Volta, it was determined that the WaPOR product [FAO, 2018] was the most suited to calculate the actual evapotranspiration. The spatial resolution is $0.0022° \times 0.0022°$, the temporal resolution is 10 days and the temporal coverage is from 2009 to present. WaPOR takes inputs from the MODIS and the GEOS-5 instrument and calculates the soil evaporation (E), canopy transpiration (T), and evaporation from rainfall intercepted by leaves (I) separately. These values are then summed together to form the actual Evapotranspiration and Interception (ETIa) [Bastiaanssen et al., 2012] every 10 days. Checking this data into the long-term water balance is coherent, as can be seen in the Budyko framework in Figure 2.6

2.2.4 Volume/area curve

In February 2000, the SRTM30 satellite mission [Farr et al., 2007] generated a comprehensive global digital elevation map of the Earth. Subsequently, in 2013, the Bui reservoir was filled, imposing specific water level constraints of 168 MASL as the minimum and 183 MASL as the maximum. Given that the elevation map predates

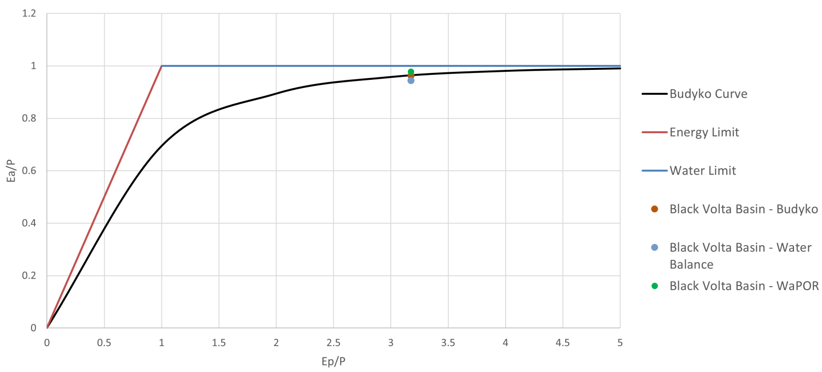

Figure 2.6: Budyko curve relation in the Black Volta Basin, the position on the graph indicates that the evaporation in the BVB is limited by the water availability

the reservoir's filling and the known design water levels, it is relatively straightforward to compute the reservoir's elevation-area-storage capacity curves using QGIS and SRTM30.

By utilizing QGIS, the area, and volume below a particular elevation can be calculated. This process was repeated for each meter between 168 MASL and 183 MASL, resulting in the generation of the volume and area curve at 1-meter vertical resolution, as depicted in Figure 2.7. Subsequently, the BPA revealed that they had previously developed a volume-area curve during a feasibility study. However, this curve possessed an accuracy increment of 10 meters and is also presented in the Figure. Notably, the slopes of the two curves are nearly identical, although the BPA curve tends to slightly overestimate compared to the SRTM curve. Due to the higher accuracy increment and slightly more conservative nature of the SRTM curve, it was deemed more appropriate for further calculations.

$$Volume = 0.089632 * h^3 - 41.312375 * h^2 + 6585.140468 * h - 358308.796 \quad (2.1)$$

$$Area = 8831808.816316 * h - 1200311111.188030 \quad (2.2)$$

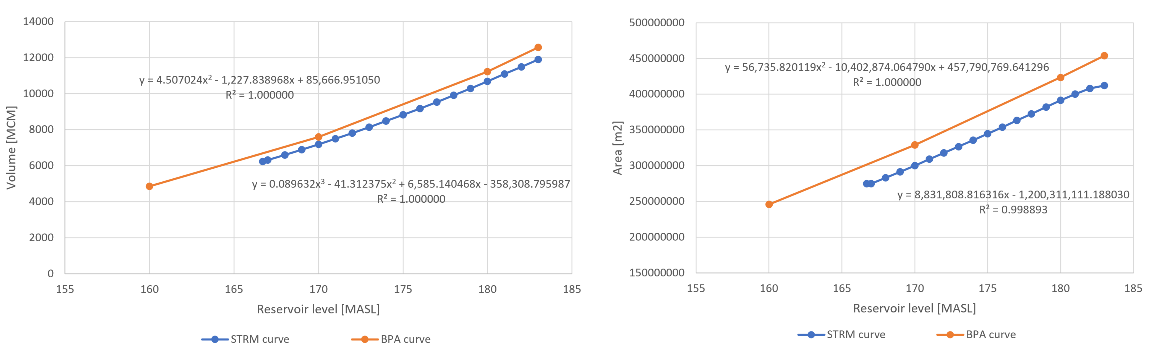

Figure 2.7: Reservoir volume curve (left) and the area curve (right) calculated using the DEM file (blue) on a 1 meter vertical scale vs the curve given by BPA on a 10m scale (orange). It can be seen that the BPA curve is slightly overestimating the SRTM curve

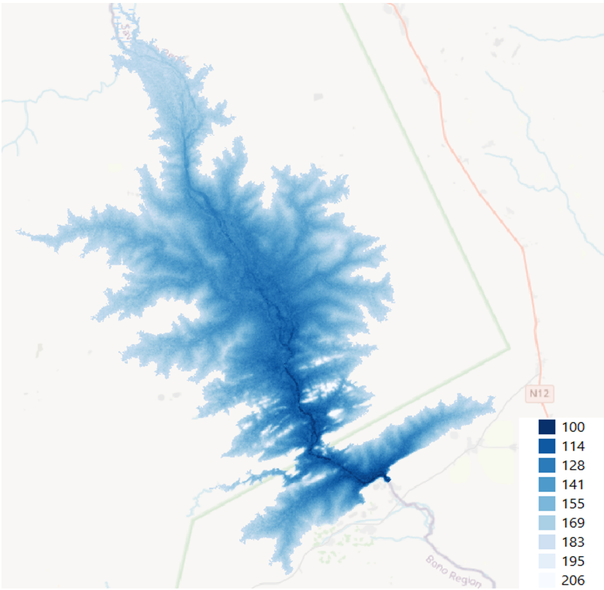

Figure 2.8: SRTM data used to calculate the reservoir volume and area curve

3 Methodology

3.1 Recalibrating the Chache rating curve

As discussed in Section 2.2.2, it is likely that the calculated discharge in Chache overestimates the actual discharge when the water level exceeds the river banks, approximately at a height of 4.6 meters. To address this issue, a recalibration is required for the rating curve to account for instances when water flows beyond the river banks. This update will involve comparing the discharge in Chache with the inflow into the reservoir and assuming that the inflow (Qinflow) into the reservoir is equivalent to the discharge in Chache. The inflow into the reservoir will be computed using the reservoir balance for the Bui reservoir (see equation 3.4).
The distance between Chache and the Bui reservoir is approximately 105 km. Along this stretch, there are several small tributaries that may not always connect to the Black Volta during the dry seasons. However, there is one significant tributary originating from Kopingue (Gbanlou) that flows into the Black Volta. Local visual estimations suggest that during the rainy season, the size of this tributary is roughly one-third of the Black Volta River. Consequently, assuming that the river discharge in Chache is equal to the inflow into the Bui reservoir represents a very conservative estimate, i.e. leaning on the safe side to avoid overestimation.

The inflow into the reservoir using the reservoir water balance is derived from the following expressions:

$$\Delta V = Q_{in} - Q_{out} \tag{3.1}$$

With: $$Q_{in} = Q_{inflow} + PREC * A_{reservoir} \tag{3.2}$$

$$Q_{out} = Q_{turbines} + AET * A_{reservoir} \tag{3.3}$$

This gives: $$Q_{inflow} = \Delta V - PREC * A_{reservoir} + Q_{turbine} + AET * A_{reservoir} \tag{3.4}$$

During the year the reservoir will either fill up or empty water depending on the balance between the inflows and the outflows. BPA measured the water level elevation every day since the commissioning of the dam. With these daily elevation measurements and the volume-area curve calculated in Section 2.2.4, the daily volume change ΔV can be calculated.

Accurate precipitation measurements are made since 2020 by TAHMO stations, BPA also keeps records of precipitation since 2018 using a bucket rain gauge.

Because the actual evaporation from the WaPOR satellite product is not able to calculate from open waters, the AET of the reservoir is determined using the simple relation AET = 0.8*PET that was determined in a paper from Shoemaker and Sumner [2006]. The PET data were derived from the MOD16 product as described in subsection 2.2.3. Although, the paper from Andreini et al. [2000] describes the actual evaporation from the Akosombo reservoir as equal to the mean potential evapotranspiration. But because the PET data from the MOD16 is already quite high compared to other PET sources, it was chosen to use the factor 0.8 from Shoemaker and Sumner [2006]. Note that the MOD16 cannot calculate PET over water surfaces so it is important to take the area around the reservoir to have the reference PET of the area. The MOD16 data goes until the end of 2021, and there is only precipitation since 2018. So the Chache rating curve will be updated using data from 2018 to 2021. In Figure 3.1, the measured Chache discharge is compared to inflow into the reservoir using equation 3.4. The data have been resampled to a 4-day period to attenuate the daily fluctuations of the reservoir balance curve. It is pleasing to observe that in the lower flows (when the water level is still lower than the river banks), the Q_{inflow} and the Chache measured discharge are really similar. And as expected, during the wettest months of the year, the Chache discharge overestimates compared to the inflow into the reservoir. The difference grows larger in the function of higher Chache discharges (compare the year 2020 with 2021). These observations confirm the hypothesis that the rating curve in Chache only correctly calculates the lower flows and updating it is necessary before using it to calibrate the hydrological model. The updated rating curve is described in Section 4.1.

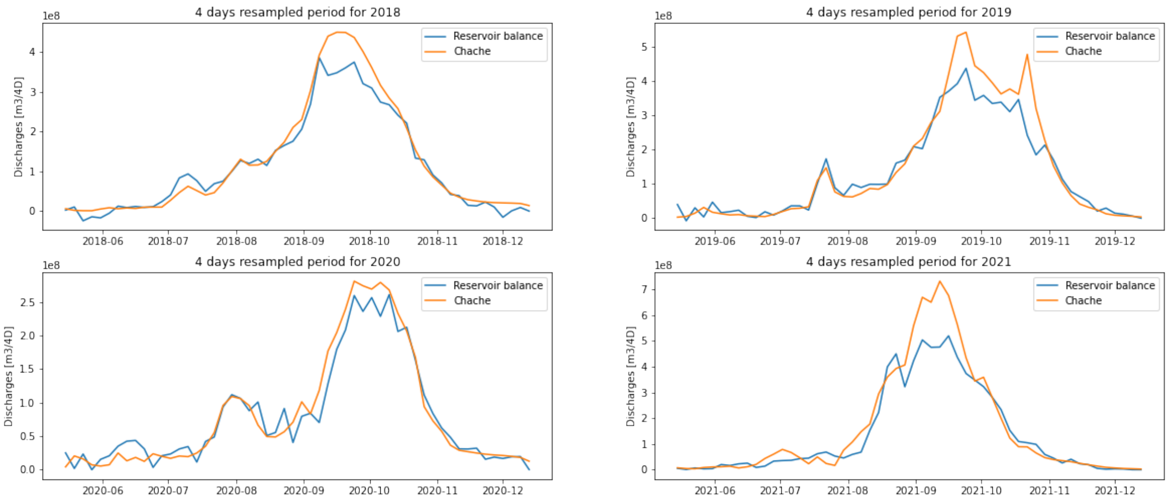

Figure 3.1: The comparison of discharge measurements in Chache with the reservoir inflow (from eq. 3.4). With 2020 being an average flow year and 2021 a high flow, the disparity increases proportionally with the wetness of the year, confirming the hypothesis

3.2 Hydrological model

Hydrological modeling plays a crucial role in environmental science and engineering, enabling the understanding and prediction of various processes. These models can vary in their representation of processes, such as conceptual versus physically-based models[Beven, 1989]. At the catchment scale, conceptual models are widely employed due to their ability to capture hydrological dynamics efficiently. These models directly describe the hydrological processes at the scale of interest based on relationships between catchment storage and outflow [Fenicia et al., 2011]. Additionally, the discretization of the physical domain can be divided into three categories of spatial model organization: lumped configuration, semi-distributed configuration, and fully-distributed configuration. The lumped configuration assumes uniformity across the entire physical domain, resulting in simple models with few parameters but the limited capability to capture spatial variations and produce distributed streamflow predictions. On the other hand, fully-distributed models, which divide the physical domain into fine grids and account for flux exchanges between neighboring grid cells, offer a more detailed representation but require a larger number of parameters and higher computational demands. The semi-distributed configuration, often implemented by discretizing the catchment into Hydrological Response Units (HRUs) assumed to exhibit similar hydrological behavior, strikes a balance between the two approaches in terms of spatial complexity and parameterization.

3.2.1 Analysing the area and defining objectives

Before starting the modeling process, it is important to gain a thorough understanding of the basin's characteristics. Table 3.2 presents an overview of the annual relationship between precipitation, discharge, and runoff coefficients.

The daily precipitation data obtained from the meteorological agency of Burkina Faso's stations (refer to Figure 2.3) was interpolated, as described in Section 2.2.1, and then aggregated on a yearly basis. This yearly precipitation of each catchment was then averaged as a function of the size of the area of the catchment.
Furthermore, the cumulative discharge in the Chache River was computed using the updated rating curve, and the resulting value was divided by the total area of the Black Volta Basin, providing discharge values in millimeters for each year. The runoff coefficient was then calculated as the ratio of the total discharge to the average precipitation. Additionally, a correlation analysis was performed between the catchment's precipitation and the cumulative discharge. From there interesting observations could be made.

Firstly, it is evident across different years that variations in average precipitation within catchments 4 and 5 do not exert a substantial influence on the discharge. This phenomenon can be attributed to the Sourou extraction, which is further discussed in Sections 2.1 and 3.2.5. Catchment 2 demonstrates the strongest correlation with the discharge. Remarkably, although the year 2022 exhibited the highest discharge, it ranked only 11th in terms of average precipitation. However, it represented the second-highest yearly precipitation within catchment 2. Conversely, in 2019, the highest average yearly precipitation and greatest yearly precipitation in catchment 2 were observed, yet it ranked as the fifth-largest discharge event. This disparity between 2022 and 2019 underscores the significance of rainfall distribution throughout the year. In 2022, there were exceptionally wet months in August and September, whereas 2019 experienced a more evenly distributed pattern over the months with an unusually wet month of October.

The modeling challenge lies in the ability of the model to distinguish between various types of rainfall characteristics while accurately simulating discharge. The primary objective of the modeling effort is to effectively capture the dynamics of high flows and peak events.

Year	Catchment 5	Catchment 4	Catchment 3	Catchment 2	Catchment 1	PREC Average [mm]	Discharge Sum [mm]	RC [-]
2000	1068	427	697	1060	1173	817	26.85	0.033
2001	936	597	775	925	960	810	19.77	0.024
2002	869	547	722	811	915	749	17.75	0.024
2003	1167	725	1034	1075	1102	999	42.15	0.042
2004	845	519	826	862	1100	803	23.52	0.029
2005	776	571	714	775	881	727	15.97	0.022
2006	1073	673	840	1035	1142	915	31.17	0.034
2007	1015	597	861	853	866	824	58.25	0.071
2008	1070	555	961	1030	973	892	56.93	0.064
2009	1031	697	824	1011	1253	924	12.89	0.014
2010	1122	752	1027	1115	1086	999	61.28	0.061
2011	845	557	808	842	938	780	nan	nan
2012	1191	712	1012	1055	989	973	nan	nan
2013	1066	550	868	889	926	837	30.97	0.037
2014	1095	586	993	1066	1047	930	33.92	0.036
2015	1101	845	940	1082	994	976	48.55	0.050
2016	1044	594	941	1132	1041	915	36.79	0.040
2017	849	636	884	809	800	797	22.50	0.028
2018	1168	614	955	1201	1335	1001	51.47	0.051
2019	1172	712	1076	1288	1249	1060	57.52	0.054
2020	1122	598	827	977	996	869	35.76	0.041
2021	1153	608	845	1126	1230	939	62.46	0.067
2022	849	653	870	1252	1183	915	74.13	0.081

Figure 3.2: Interpolated precipitation over each catchment using the Thiessen method and data from the meteorological agency of Burkina Faso. Discharge data is calculated from the updated rating curve and divided by the total sum of the area. Missing discharge data in 2011 and 2012 due to the construction of the dam

3.2.2 SuperflexPy

SuperflexPy is a versatile open-source Python framework [Dal Molin et al., 2021] that offers flexibility in constructing conceptual hydrological models using the SUPERFLEX principles described in Fenicia et al. [2011]. It is specifically designed to accommodate models with diverse levels of structural complexity and supports a wide range of spatial configurations, from a simple lumped reservoir to a distributed catchment. SuperflexPy is a Python package that empowers modelers to maximize the capabilities of the framework seamlessly, eliminating the requirement for separate software installations. This integration simplifies the usage of SuperflexPy and facilitates easy interfacing with existing Python code for easier model deployment.

Numerical implementation

Reservoirs are controlled by ordinary differential equations (ODEs) that cannot be solved analytically. Therefore SuperflexPy incorporates various numerical approximators and root finders to enhance the modeling experience. The available numerical approximators include implicit and explicit Euler methods, as well as the Runge-Kutta 4 method. Additionally, the framework offers three root finders: one implementing the Pegasus method, one utilizing the Newton method, and another specifically designed for explicit algebraic equations. The SuperflexPy environment also offers the possibility to create and implement customized numerical approximators and root finders. For optimal performance, it is recommended, based on previous modeling studies with the SUPERFLEX framework, to employ the Implicit Euler approximation and the Pegasus root finder [Dowell and Jarratt, 1972][Fenicia et al., 2011]. It is a configuration that ensures robust solutions for the ODE.

3.2.3 Model descriptions

The selection of model hypotheses in this study is motivated by several considerations:

1. The type of system and associated dominant processes including prior insights into the catchment characteristics previously described in Section 2.1. The model performance is related to signatures of aridity and baseflow, in this case: high aridity with low baseflow.
2. Previous hydrological modeling in the area from different papers such as Kwakye and Bárdossy [2020], Shaibu et al. [2012], Sawai et al. [2014] and Akpoti et al. [2016].
3. The (limited) data availability.
4. The objective of the application: model the high flows and some individual peaks on a daily temporal scale.

Conceptual models can be divided into three different structures: single (M1), serial (M2 & M3), and parallel (linear and non-linear: M4 & HBV) structures, see Figure ref3.3. When the model is cast in this form, it is described as a state-space representation. A state-space representation is a mathematical model of a physical system as a set of input, output, and state variables related by first-order differential equations.

In the context of this research five different model hypotheses (all using the SUPERFLEX configurations) of varying complexity are considered, see Figure 3.3. Due to the data scarcity, it was chosen to lump the models over each sub-catchment. All the models aim to replicate the overall discharge for each individual sub-catchment by utilizing observed precipitation and pre-estimated actual evaporation (Ea). It was chosen to use actual evaporation instead of potential because the Ea was deemed reliable because of the long-term water balance. Additionally removing two parameters in the model which accounted for the change of potential to actual evaporation.

The SUPERFLEX models in Figure 3.3 consists of up to four reservoirs, conveniently labeled as "fast" (FR), "slow" (SR), "unsaturated" (UR) and "interception" (IR) serving different purposes. Furthermore, three models M3, M4, and HBV incorporate a lag function to account for flow network routing delays. The mathematical equations governing the models are described in the Section 3.2.4.

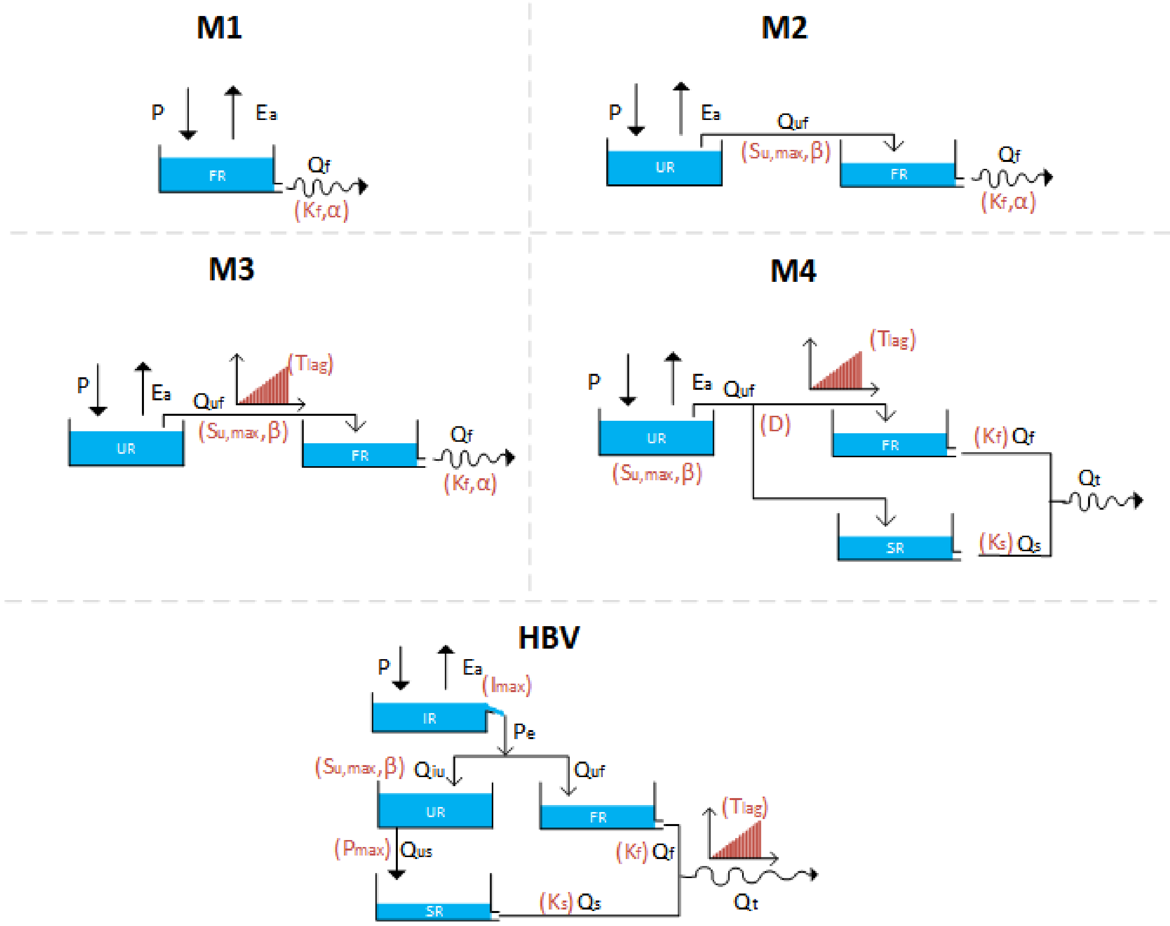

Figure 3.3: Overview rainfall-runoff models calculating the discharge output for each sub-catchment, all the models were made using SuperFlexPy. The parameter for each model are illustrated in red

M1: 1-bucket model (non-linear reservoir)

The simplest model, M1, represents catchments as "simple dynamical systems" by using a single power law reservoir to simulate both catchment streamflow and evaporation. This model considers streamflow to be determined solely by the total water storage of the catchments. The water is drained as fast lateral recharge and is routed through a fast responding lateral flow path component SF [mm] with a storage coefficient K_f [d^{-1}] and released as preferential flow Q_F [mm/d] to the stream. Despite its simplicity, various research [Kirchner, 2009] has shown that even this basic model can yield accurate streamflow simulations in certain catchments. This model has two parameters (K_f and α).

M2: 2-bucket model

The second model incorporates two separate components ("buckets"), to differentiate between fast flow and unsaturated flow. The unsaturated flow is represented by a power function that depends on the storage. Specifically, the unsaturated flow component involves an unsaturated root-zone storage reservoir, denoted as S_u [mm], which has a maximum storage capacity represented by $S_{u,max}$ [mm]. $S_{u,max}$ represents the maximum volume of water stored in the soil pores between the field capacity and the permanent wilting point, which is accessible to plant roots. This model has four parameters (K_f, α, $S_{u,max}$ and β).

M3: 2-bucket model with time-lag

M3 differs from M2 by the addition of a half triangular lag function (more explanation in Section 3.2.4 to the flow that connects the unsaturated reservoir and the fast reservoir. This model has five parameters (K_f, α, $S_{u,max}$, β, and $T_{lag\ ,max}$).

M4: 3-bucket model with time-lag

M4 and M5 differ in terms of their reservoir configurations. M4 includes an extra reservoir, known as SR, which represents a groundwater component and simulates slow flow. The relationships governing the unsaturated flow (UR) and fast flow (FR) in M4 are nonlinear. Additionally, the allocation of water to the SR reservoir is determined by parameter D. In total, M4 consists of six parameters (K_f, α, $S_{u,max}$, β, $T_{lag\ ,max}$ and D).

HBV-model

The HBV model is a lumped conceptual catchment model that has eight model parameters and takes precipitation and evapotranspiration as forcing inputs. The incoming water in the system is the precipitation P, it can evaporate from the interception reservoir Si at the potential rate Ei . Once the interception reservoir reaches the maximum storage capacity Imax water will spill as effective precipitation Pe from the interception reservoir to the unsaturated rootzone Su and to the fast-responding lateral flow path Sf. Water from the fast reservoir Sf is released as preferential flow Qf. The water from the unsaturated rootzone will percolate to the groundwater at a rate determined by the probabilistic approach using the concept of a runoff coefficient Cr. Next, the groundwater reservoir releases water as groundwater flow Qs. Lastly, Qf and Qs are summed and routed through the half-triangular transfer function with a time lag. The parameters in the HBV model are: K_f, K_s, β, $S_{u,max}$, I_{max}, P_{max}, C_r, and $T_{lag,max}$).

3.2.4 Mathematical equations

Fast and slow reservoir

The fast reservoir, common in hydrological models, assumes that the storage-discharge relationship is described by a power function. The behavior of the reservoir is defined by the mass balance equation:

$$\frac{dS}{dt} = P - Q$$

With: P = precipitation and Q= discharge

The discharge in the above mass balance equation can be expressed as a function of stored water in the reservoir

$$Q = K_f * S^{\alpha} \tag{3.5}$$

With: K_f = storage coefficient [1/d], S = storage state [mm]

The slow reservoir assumes a linear storage-discharge relationship. It is used in the model to simulate lower-zone storage processes.

$$Q = K_f * S \tag{3.6}$$

Unsaturated reservoir

The unsaturated reservoir in a conceptual hydrological model represents the storage and movement of water in the soil's unsaturated zone. This zone lies above the water table and contains both air and water, with the water content below its maximum capacity. The reservoir accounts for processes such as infiltration, percolation, and drainage. It captures the interactions of precipitation, evaporation, and soil moisture dynamics.

$$\frac{dS}{dt} = P - E_{act} - Q$$

$$\bar{S} = \frac{S}{S_{max}} \tag{3.7}$$

$$Q = P * (\bar{S})^{\beta} \tag{3.8}$$

Half triangular lag

SuperflexPy's lag elements have the capability to handle any number of input fluxes and utilize a convolution-based approach with a weight array that defines the lag function's shape. The lag elements only differ in the specific definition of their weight arrays. The inputs and outputs of the lag elements depend on the preceding element in the sequence. The weight array can be determined by specifying the area beneath the lag function relative to the time coordinate [Fenicia et al., 2011]. For this research, it was chosen to use the half-triangular. It is a simple but efficient function that exhibits linear growth until reaching a certain time (t_{lag}), after which it falls to zero, as illustrated in Figure 3.4. The slope parameter (alpha) of the triangle is determined to ensure that the total area under the function is equal to 1.

$$\begin{aligned} A_{lag}(t) &= \alpha * t && for\ t \leq t_{lag} \\ A_{lag}(t) &= 0 && for\ t < t_{lag} \end{aligned}$$

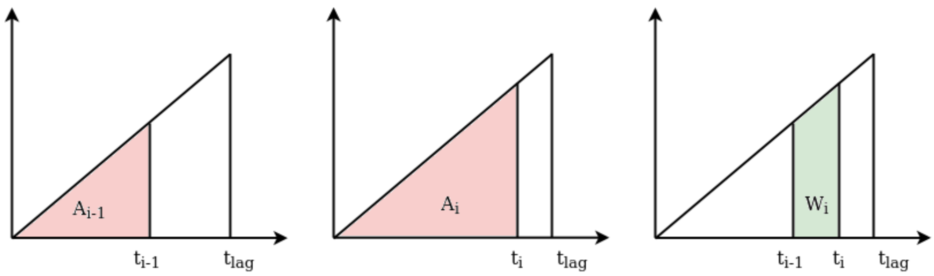

Figure 3.4: Half triangular lag function (source: SuperflexPy [Fenicia et al., 2011])

3.2.5 Modeling the Sourou Extraction

The Sourou depression, discussed in Section 2.1, presents a rare occurrence where a river changes its direction of flow for a specific period [Shahin, 2003]. During the wettest months of the year, the Sourou diverts water from the Mouhoun River instead of flowing in. Despite limited available information regarding the specifics of this phenomenon, valuable insights can be obtained from the Global Runoff Data Centre (GRDC) (Section 2.2.2 [Centre, 2019]). From there data of the mean monthly discharge data collected from 1956 to 1982 at two stations, 'Kouri' upstream of the intersection and 'Manimenso' downstream of the intersection, sheds light on the river's characteristics. The data was initially gathered during the First GARP Global Experiment (FGGE). It likely followed the same measurement protocols as a study preparation for the construction of a regulation mechanism with a storage capacity of $250*10^6$ m^3 in the village of Léry in 1984 [Bro, 2001]. By analyzing the data from Figure 4.3, it can be observed that only during the wetter years, the discharge is diverted from the Mouhoun. The challenge is to determine at which moment and in which condition this happens and how could this phenomenon be reciprocated in the hydrological model. This was done in Section 4.2.1.

3.3 Calibration

The challenge of making hydrological models is to establish a quantitative link between the system input, the system state, and the system output. Every model that can be used is a hypothesis and is at best an incomplete description of reality. Every physical system consists of multiple interacting components of different scales. It is hard to identify which parameters are correct. Therefore model development is a continuous process of testing alternative model hypotheses. The models make use of the top-down approach and are a combination of conceptual models and data-driven models. This means that fewer data and model parameters are required in comparison to the bottom-up approach. However, the spatial resolution is lower and the physics is simplified. The result will not be one right model, but a range of different models with different system states, which have the best approximation of the reality.

The available discharge data for the catchment, along with corresponding precipitation data, is limited to the downstream Section. This poses a challenge when it comes to determining and calibrating the parameters for the various upstream catchments. Several papers have addressed this issue and explored calibration techniques in data-scarce environments. One particularly helpful paper on this topic is the research done by Hulsman et al. [2020]. It provides valuable insights into different approaches for calibrating models in regions with limited data, primarily utilizing various satellite products. Following the strategy described in the above-mentioned paper, the first step is narrowing down the feasible parameter range involves utilizing data from the Gravity Recovery and Climate Experiment (GRACE), which captures seasonal fluctuations in total water storage. Secondly, altimetry data is then employed to further refine the parameter set, this method focuses more on the river dynamics.

It's important to note that due to limited data availability and equifinality [Savenije, 2001], the goal is not to find the optimal parameter. Instead of risking the rejection of valid parameter sets [Hrachowitz and Clark, 2017], the calibration focused on identifying and excluding the most implausible sets inconsistent with the available data. To achieve this, a Monte Carlo sampling technique with uniform prior parameter distributions were used for each method and sub-catchment, generating 10,000 model realizations. These random solutions served as a starting point and were then progressively refined by identifying parameter sets that did not meet the conditions. This iterative approach narrowed down the range of feasible parameters for each sub-catchment and, consequently, reduces uncertainty in the modeled hydrograph [Hrachowitz et al., 2014].

3.3.1 Parameter selection based on the seasonal water storage: GRACE

The observations GRACE provides mean monthly data on anomalies in total water storage. These anomalies encompass all forms of terrestrial water, including groundwater, soil moisture, and surface water. By monitoring variations in the Earth's gravity field using two identical satellites, regional changes in mass can be detected, with terrestrial water storage being the primary driver once atmospheric effects are considered [Landerer and Swenson, 2012]. The data was downloaded from the GRACE database provided by the University of Texas Center of Space Research (UT-CSR) release 06 monthly solutions filtered with DDK5 [Ries et al., 2016].

As described in Hulsman et al. [2020], this data was then compared using the Nash-Sutcliffe efficiency [Nash and Sutcliffe, 1970] between the monthly modeled total water storage of each different model described in Section 3.2.3. The following equations were used for each model $S_{tot,M1} = S_f$, $S_{tot,M2\&M3} = S_u + S_f$, $S_{tot,M4} = S_u + S_f + S_s$, *and* $S_{tot,HBV} = S_u + S_f + S_s + S_i$. The Nash-Sutcliffe Efficiency (NSE) is defined as:

$$NSE = 1 - \frac{\sum_{i=1}^{n}(\theta_{obs,i} - \theta_{mod,i})^2}{\sum_{i=1}^{n}(\theta_{obs,i} - \bar{\theta}_{obs})^2} \tag{3.9}$$

where: NSE is the Nash-Sutcliffe Efficiency, $\theta_{obs,i}$ represents observed values, $\theta_{mod,i}$ represents predicted values, n is the total number of observations, and $\bar{\theta}_{obs}$ is the mean of the observed values.

3.3.2 Parameter selection based on satellite altimetry data

In this calibration methodology, the direct utilization of altimetry data was employed to establish a correlation between the observed water levels derived from virtual stations and the modeled discharge [Seibert and Vis, 2016]. This approach is predicated upon the assumption that the relationship between water level and discharge exhibits a monotonic trend [Hulsman et al., 2020]. The altimetry data utilized in the Black Volta basin was obtained from the Database for Hydrological Time Series of Inland Waters (DAHITI) [Schwatke et al., 2015]. For the calibration process, three virtual stations were selected: one located within catchment 5, another positioned slightly downstream after the intersection of the Sourou and the Mouhoun rivers, and a third downstream of catchment 3. The water level data spans from 2016 to the present and is available at a frequency of approximately once per month. Unlike GRACE, which provides mean monthly values, the altimetry data represents a single measured value of water level once a month when the satellite passes overhead. Due to the lack of knowledge regarding the characteristics of the river between the two satellite measurement points, the evaluation of the model using the Nash-Sutcliffe efficiency (NSE) metric is not suitable. Instead, the altimetry data and discharge are transformed into a relative scale (with the minimum value equal to 0 and the maximal value equal to 1). Then the relative error is computed (with 1 being a perfect match) by comparing the relative measured water level obtained from altimetry data with the relative modeled discharge for the corresponding day, and not by resampling the data to a monthly scale. This approach focuses exclusively on the river dynamics rather than considering the volume.

During the calibration phase using the altimetry data, it was observed that the Monte Carlo sampling technique could lead to the generation of unrealistic discharge values within the optimal parameter ranges. These values were sometimes either excessively large or small, this is a consequence of working on a relative scale. To address this issue, an additional constraint was introduced, namely the runoff coefficient. The runoff coefficient represents the proportion of rainfall water transformed into runoff and is calculated as the ratio of the total discharge to the total precipitation over the course of a year. By incorporating a range of "realistic" runoff coefficients as a constraint in the parameter calibration process, the parameter set could be further constrained. The value of the runoff coefficient is influenced by the specific land cover types present in the area. For instance, regions with land use and water bodies tend to exhibit higher runoff coefficients due to their limited capacity for water infiltration. Conversely, grasslands, shrubs, and forested areas generally display lower runoff coefficients. Changes in runoff coefficients are primarily driven by the expansion of urbanization and agricultural land use [Akpoti et al., 2016]. However, since the size of each catchment is considerable, it is assumed that these effects are mitigated to some extent.

3.3.3 The final calibrating process

The main idea behind the final calibrating process is the self-proclaimed: "upstream to downstream check-point approach". In summary, the model calculates the output starting from the most upstream catchments. Controls if the calculated values are realistic by passing a checkpoint and if it is, the model proceeds to calculate the output for the downstream catchments, and so on. This approach aims to find the optimal parameter combination range and can be explained in the following steps:

Step 1: Define the parameter range.

Step 2: Calculate a random value within the given range for each parameter and calculate the model output for each sub-catchment.

Step 3a: Calculate the runoff coefficient for catchment 5. If it is within the realistic runoff coefficient range, continue, else go back to Step 2.
3b: Calculate the relative error based on the altimetry data for catchment 5 from virtual station 24873 (see Figure 2.3). If the error is above a defined threshold, continue; otherwise, go back to Step 2.

Step 4. Calculate the updated output of catchment 5 and catchment 4 as a result of the Sourou depression, as described in Section 4.2.1.

Step 5a: Calculate the runoff coefficient with the updated output of catchment 5 and catchment 4. If it is within the realistic runoff coefficient range, continue; otherwise, go back to Step 2
5b: Calculate the relative error based on the altimetry data from virtual station 24871 for the updated output of catchment 5 and catchment 4. If the error is above the threshold, continue; otherwise, go back to Step 2

Step 6a: Calculate the runoff coefficient for catchment 3. If it is within the realistic runoff coefficient range, continue; otherwise, go back to Step 2

6b: Calculate the relative error based on the altimetry data from virtual station 12234 for the total output of catchment 3, 4, and 5. If the error is above the threshold, continue; otherwise, go back to Step 2

Step 7: Calculate the runoff coefficient for catchment 1 and 2. If it is within the realistic runoff coefficient range, continue; otherwise, go back to Step 2

Step 8: Calculate the total output as the sum of the output of all the catchments at the Checkpoint

Step 9: Compare the total model output with the measured discharge using the Nash-Sutcliffe efficiency. If the value is above a defined threshold, save the parameter set

Step 10: Study and process the parameter set to narrow down the range of realistic values defined in Step 1

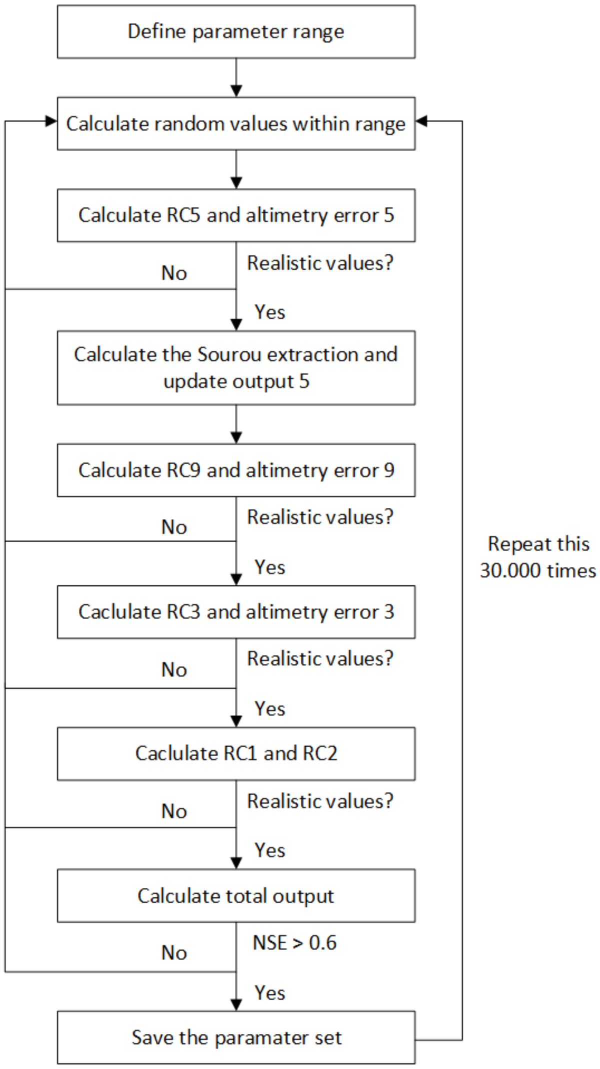

Figure 3.5: The calibrating process "upstream to downstream check-point approach"

4 Results and discussion

4.1 The recalibrated Chache rating curve

4.1.1 Results

The main assumption about the method of recalibrating the rating curve was to assume that the reservoir inflows, calculated from the reservoir balance (equation 3.4), equal the discharge in Chache (105km upstream of the reservoir). This was done over a period from 2018 to 2021, this limited amount of years is due to the lack of precipitation data in that area. During that period the water level in Chache was measured every day and converted to discharge in [m^3/s] using the following rating curve (obtained from BPA):

$$Q_{old} = C * (h + a)^m = 21.5 * (h - 0.55)^{2.4} \tag{4.1}$$

Where:

Q : Discharge (in m^3/s)

C : Rating curve coefficient

h : Measured water level

a : Offset or constant term

m : Exponent of the rating curve

Next, the calculated discharge from the water balance was then associated with the water level on that same day, and a rating curve was fitted, see Figure 4.1. In this Figure, the old rating curve and the updated one determined using the reservoir balance are compared. It can be seen that the new rating curve returns lower discharges for higher water levels, again confirming the hypothesis.

The formula for the updated rating curve is:

$$Q_{new} = C * (h + a)^m = 20 * (h - 0.32)^{2.27} \tag{4.2}$$

From Figure 4.1, the updated rating curve makes sense because when the water flows in the river banks i.e. approximately lower than 4.6 meters, the rating curves between the old and the new one are almost identical. But when the water flows above the banks, the difference grows bigger. For the same water level, the discharge is smaller with the updated curve. The higher the water gets, the bigger the difference between the results.

Lastly, the calculated discharge with the reservoir balance and the old and new rating curve was again plotted in Figure 4.2.

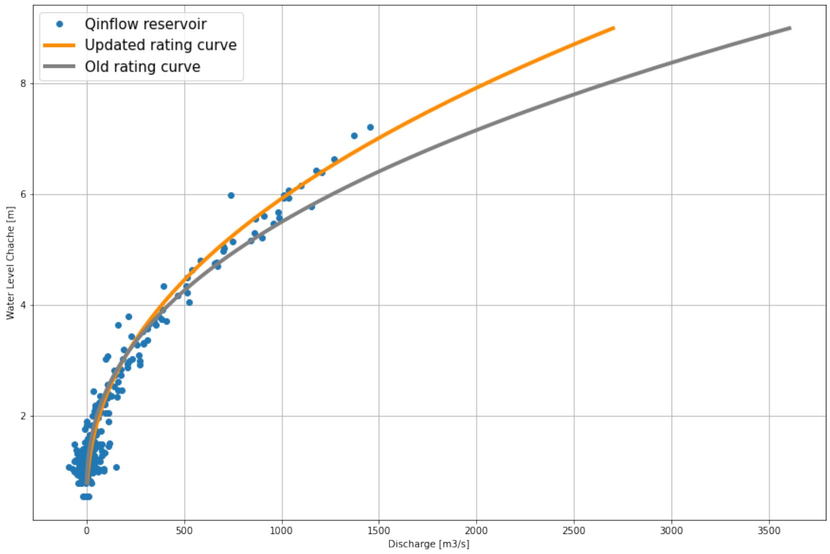

Figure 4.1: Chache rating curves comparison. In this Figure, the old rating curve and the updated one (fitted in the function of the reservoir inflows (blue dotts)) are compared. It can be seen that the new rating curve returns lower discharges for higher water levels

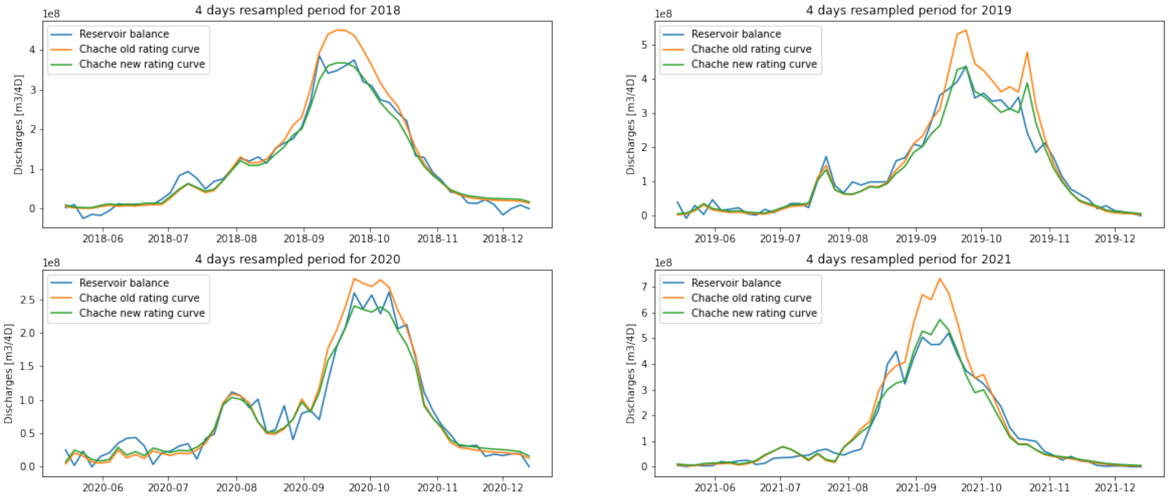

Figure 4.2: Comparing the inflows of the reservoir balance at a 4-day resampled scale with the updated discharges from Chache

4.1.2 Discussion

As explained earlier the Chache and Bui reservoir are separated by a distance of 102 km. Along this stretch, there exist several small tributaries that, during certain dry seasons, may not even connect to the Black Volta River. However, there is a larger tributary originating from Kopingue (Gbanlou) that flows into the Black Volta. According to local visual estimations, the size of this tributary is approximately one-third of the Black Volta River during the rainy season (approximately confirmed using satellite imagery from Google Maps). Additionally, the volume-area curve also is made using a conservative approach as described in Section 2.2.4. Therefore, assuming that the river discharge in Chache is equivalent to the inflow into the Bui reservoir is a highly cautious approach. In the rainy season, due to all the tributaries, the inflow in the reservoir is without a doubt higher than the discharge in Chache. Because of this conservative approach, it was deemed appropriate to use the updated rating curve in the calibration and testing of the hydrological model and for future use by the Bui Power Authority.

4.2 Hydrological model

4.2.1 Results of the Sourou Extraction

Through an examination of the data presented in Figure 4.3, illustrating the discharge in Kouri, laying right upstream of the intersection between the Mouhoun and the Sourou rivers, and Manimenso, just downstream of the intersection. It becomes evident that the diversion of discharge from the Mouhoun River occurs during years with higher precipitation levels. The task at hand is to identify the specific timing

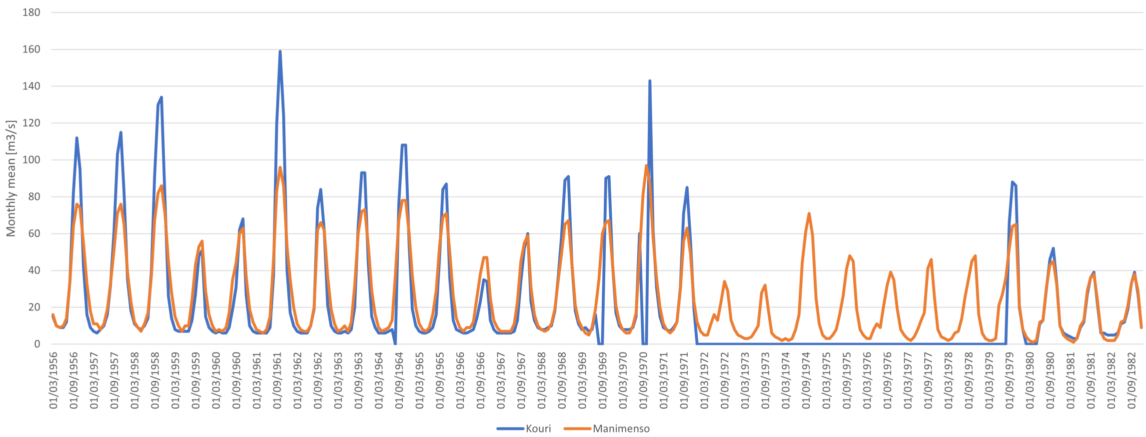

Figure 4.3: Mean monthly discharge data of Kouri, representing the discharge of the Mouhoun before the extraction, and Manimenso, just downstream of the intersection, is the discharge of the Mouhoun after the extraction

and conditions under which this phenomenon takes place and subsequently incorporate it into the hydrological model. This was done by calculating the cumulative discharge of the river for each year until the moment where the discharge of Kouri is bigger than the one Manimenso i.e. when where there is an extraction by the Sourou river. By calculating the average of the cumulative values across different years, the threshold at which the Sourou extraction takes place was determined to be at the cumulative discharge of $271*10^6$ m^3. From this moment a percentage of flow needs to be deduced from the Mouhoun to account for the Sourou extraction. Again that factor was calculated from the GRDC data as no information is available on that matter. For each month where there was a Sourou extraction, the relative difference between Kouri and Manimenso was calculated. Sourou extraction only happens during the wetter months of September, October, and November, the average percentage extraction is then respectively 17.4%, 29.5% and 25.3% per month. These factors were applied to the output of catchment 5 and obviously, during that time the output of catchment 4 into the Mouhoun goes to zero.

4.2.2 Choosing the hydrological model

Firstly, an examination of the seasonal water storage using GRACE data, as explained in Section 3.3.1, was conducted individually for catchments 1, 3, and 4. The selection of these particular catchments was predicated on their geographical distribution, encompassing the wetter southern region and the drier Sahel in the northern area. The assessment of seasonal water storage was contingent upon the availability of data spanning the years 2019 to 2021, and the results are illustrated in the figure 4.4. The outcomes indicate that model configurations M2, M3, and M4 produced the most favorable and accurate results.

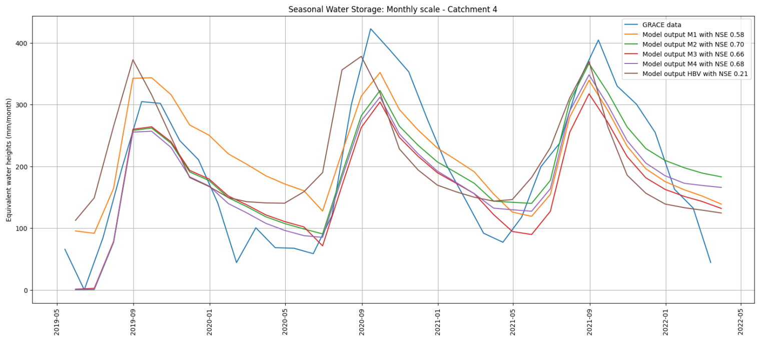

Figure 4.4: Seasonal water storage - catchment 4

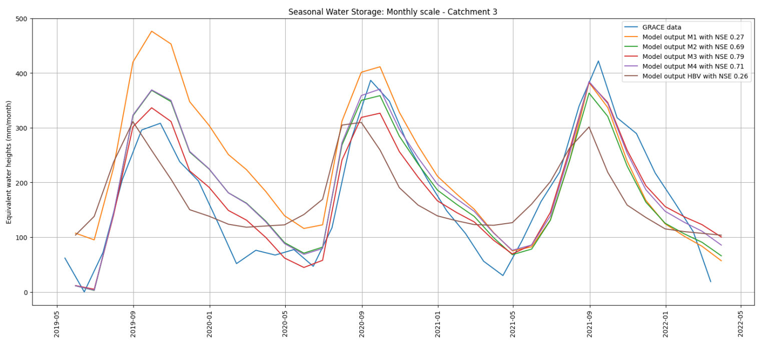

Figure 4.5: Seasonal water storage - catchment 3

The individual selection of the model based solely on altimetry did not yield significant insights due to its reliance on relative scale testing. This process introduced certain calibrated parameters that produced results at an inappropriate scale, limiting its effectiveness. However, a more promising approach emerged when catchments 5, 4, 3, and 2 were lumped into a single unified catchment. By employing the distinct model configurations illustrated in Figure 3.3 and comparing the results against the Lawra discharge, a more robust assessment was achieved.

The evaluation encompassed the examination of various datasets from different years, with Figure 4.7 displaying results for the years 2013 to 2014 to maintain clarity. Consistently and superiorly performing models were identified, specifically Model M3

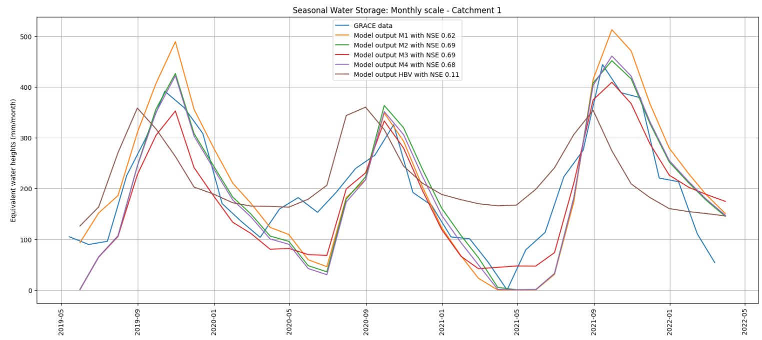

Figure 4.6: Seasonal water storage - catchment 1

and the HBV model. However, looking more into the character of the outputs of the HBV model, it can be observed that the model consistently generates smooth curves, which are deemed less suitable for this research, primarily due to its limitations in modeling sudden individual peaks. Additionally, the HBV model exhibited inaccuracies in the GRACE comparison as depicted in the above figures. Consequently, Model M3 was selected as the more appropriate model for subsequent analyses within each catchment in this study.

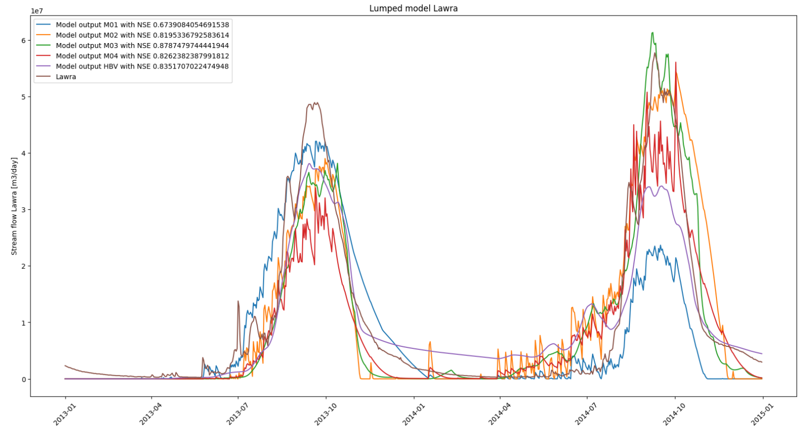

Figure 4.7: Different models results from lumping the catchments and comparing it to the Lawra discharge, model M3 and HBV gave the most consistent and accurate results

4.2.3 Calibration results

The altimetry data range from 2016 to 2022. The year 2017 is a low flow year, which is not the objective of the model and to limit the calibration processing time, the calibration period was set from 2018 to 2022. This period includes the two years of interest, 2019 and 2022, ensuring that the model adequately calibrates based on these high flows. The calibration process, described in Section 3.3.3 and depicted in Figure 3.5, involved a Monte Carlo sampling of 12,000 loops. From this calibration process, the results were narrowed down to a feasible range, defined by an NSE >0.80 (refer to Figure 4.9). The highest calibration result achieved for the calibration period from 2018 to 2022 was 0.85 (see Figure 4.10).

The results from the calibration process gave the following parameter range for model M3:

	Catchment 1	Catchment 2	Catchment 3	Catchment 4	Catchment 5
S_{max} [mm]	750-1500	700-1500	1000 - 2000	700-1750	1400 - 1800
β [-]	1.5-3.0	2.2 -3.5	1.6 - 3.5	1.1-3.0	1.75 - 3.0
Tlag,max [d]	1-25	15 -35	10 - 35	35-50	20 - 50
K_f [1/d]	0.3-0.55	0.1-0.65	0.45 - 0.9	0.1-0.6	0.1 - 0.6
α [-]	0.5-2.5	1.9-2.9	1.0 - 3.0	0.2-1.25	0.1-1.5

Table 4.1: Parameter range

The unexpectedly wide range of maximum time lags prompted a time-lag correlation analysis. This analysis involved calculating the correlation between the Chache River's discharge and the lagged precipitation for each catchment. By examining the results in Figure 4.8, it can be observed that the maximum time-lag ranges from 20 to 50 days, depending on the specific catchment. This finding aligns with the previously obtained calibration results, providing further confirmation.

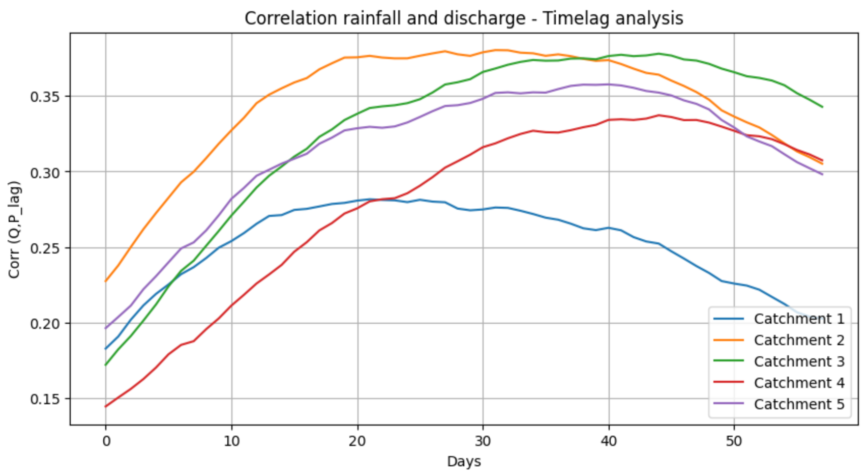

Figure 4.8: Timelag correlation analysis, the maximum range of each plot gives an idea of the lag time of each catchment

The primary objective of Model M3 is to simulate the discharge by utilizing precipitation as an input. Consequently, it is necessary for Model M3 to adequately capture the lag between precipitation (P) and discharge (Q). While the unsaturated reservoir (UR) component does not introduce any lag, and the fast reservoir (FR) component, though introducing some lag, primarily focuses on fitting the recession phase of the hydrograph. Thus, the triangular lag function is primarily responsible for fitting the lag. This lag function accounts for the overall time lag, irrespective of its underlying causes. It is important to consider the lag function and the fast reservoir as a unified component that shapes the effective rainfall (i.e. the rainfall that produces streamflow), and that accounts for all kinds of routing processes. It is and remains a lumped model for each catchment, which lumps many processes.

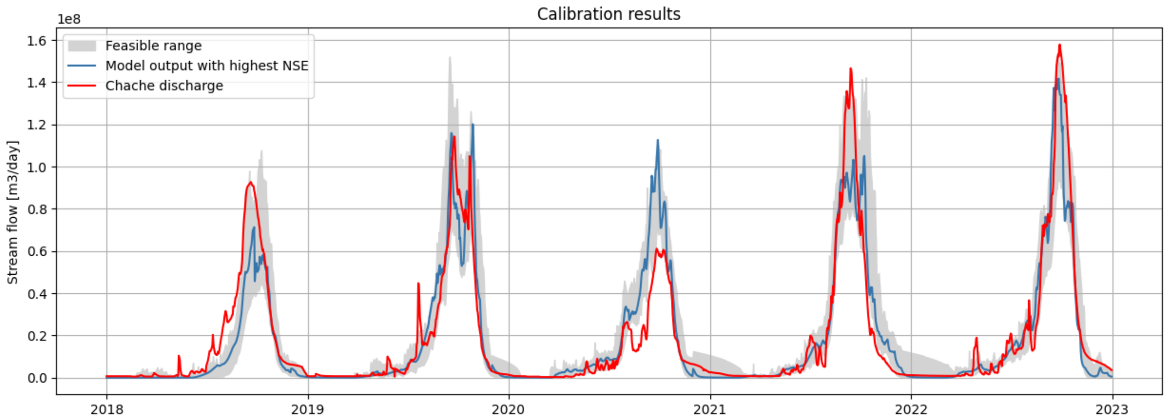

Figure 4.9: Calibration results: The feasible range in 2020 exhibits some overestimation, but overall the results are great

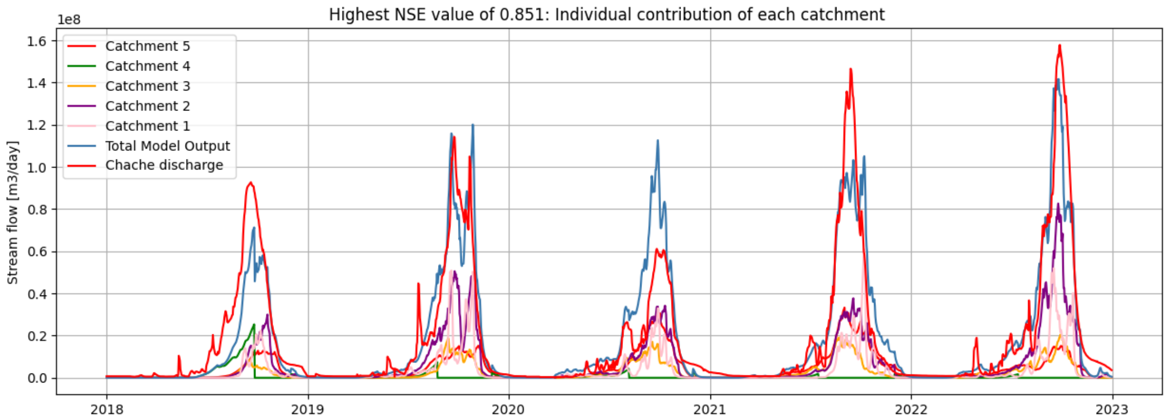

Figure 4.10: Calibration results: individual contribution of each catchment

Analysis calibration results

Upon examining the feasible range in Figure 4.9, it is observed that the year 2020 (characterized as an average flow year, see Figure 3.2) was overestimated, while all the other years (high flow years) exhibited correctly spanned discharge values.

Analyzing the individual contributions that led to the best result in Figure 4.10, several observations can be made. Firstly, for catchment 4, each year shows a sudden drop indicating the onset of Sourou extraction, followed by an increase at the end of the year, indicating the return flow from Sourou into Mouhoun. Secondly, catchment 2 has a significant impact on the total model output despite its smaller area (representing only 13% of the total area). Moving on to Figure 4.11, a closer examination was conducted on the hydrographs of the years 2019 and 2022 to better understand their characteristics. In 2019, the spill was primarily caused by an unexpected and very sudden increase in Chache. Modeling this ”double peak” was an important objective, and the model successfully captured it, as evident in the Figure, with an individual year NSE of 0.89. Correctly modeling the year 2022 presented another significant challenge due to the unusual distribution of rainfall runoff. Although it was the wettest year, with a 19% increase compared to the previous wettest year, it ranked

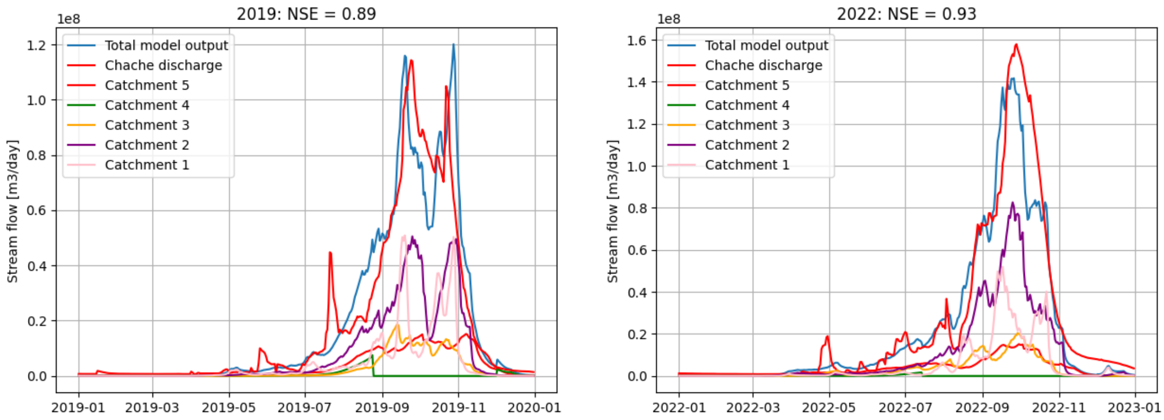

Figure 4.11: Zooming in the calibration results of the individual years causing spills

only fifth in terms of cumulative rainfall. However, the model successfully captured the dynamics of this year, achieving an NSE of 0.93.

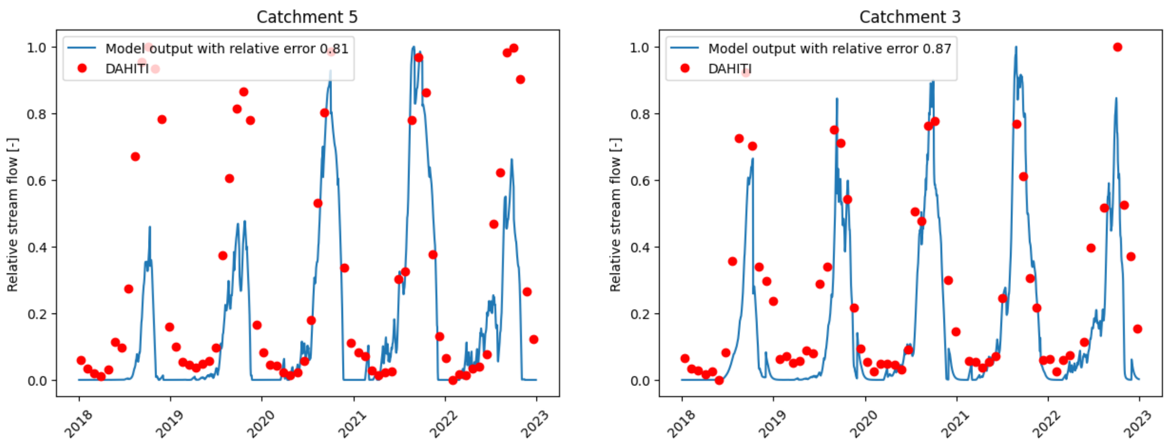

Figure 4.12: Calibration results: the individual output of catchment 5 (left) and the total output of catchments 5, 4 and 3 (right) compared to the altimetry data

4.2.4 Testing results

Independent test period

A crucial step in evaluating the model's performance is to assess it against an independent test period, without further recalibration. Only based on the results in the test period, a decision can be made if the model (and its parameters) is acceptable or not. Because the actual evapotranspiration (AET) data covers the period from 2009 to the present and to ensure that the test reflects the model with the same "conditions" as the calibration period (i.e. after the construction of the dam), the testing period was set from 2013 to 2016. The results of this evaluation are presented in Figure 4.13, where the highest NSE value obtained was 0.86. This is slightly higher than the calibration period, testing results having a higher NSE than the calibration results is quite unusual in hydrological modeling. However, this can be explained due to the fact that the years 2019, and 2022 had an unusual (and thus more difficult to model) rainfall-runoff distribution, having an impact on the calibration results. Whereas the testing years 2013 to 2016 exhibited a more normal rainfall-runoff pattern.

Upon closer analysis of the results, it is observed that for the years 2013, 2014, and 2015, the model accurately captured the shape of the discharge, albeit with slight underestimation. Conversely, in the year 2016, the model tended to overestimate the discharge. However, the overall good NSE results indicate that the model is performing well.

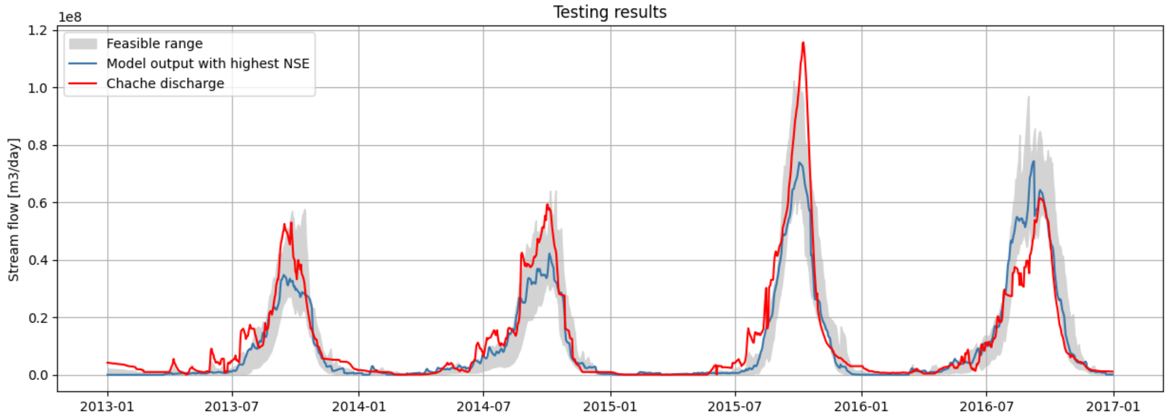

Figure 4.13: Testing results: independent time frame, without further recalibration (NSE = 0.86)

Testing with TAHMO data

Another way to test a hydrological model is to change to the input source. This was done by replacing the precipitation data from the meteorological agency of Burkina Faso with TAHMO precipitation. The TAHMO precipitation data span from 2018 to 2022 and was interpolated over each catchment using Thiessen polygons [Thiessen, 1911]. Using only TAHMO precipitation data achieves an NSE value of 0.74, as illustrated in Figure 4.14. The decline in performance can be attributed to the poor performance observed in the years 2021 and 2022, where the discharge increase commences prematurely. A more detailed analysis reveals that this issue arises from certain TAHMO stations measuring precipitation too early in the rainy season during these two years, thereby disrupting the model's functionality.

As described in Section 2.2.1, one of the significant advantages of TAHMO stations is the easy and almost immediate accessibility of measured data, typically with only a couple of hours delay after a rain event. One of the research objectives of this thesis is to explore the potential of utilizing TAHMO stations as input in the hydrological model to gain insights that can aid in reservoir management decision-making.

To test this hypothesis, the focus will be on the year 2019, which exhibited a double peak pattern due to an unusually wet October resulting in an unexpected spill. In 2019, only six out of the sixteen TAHMO stations in the Black Volta Basin (see Figure 2.4) were operational. To evaluate the potential usefulness of TAHMO stations, the model was updated, in light of occurring precipitation events, as if it were in October

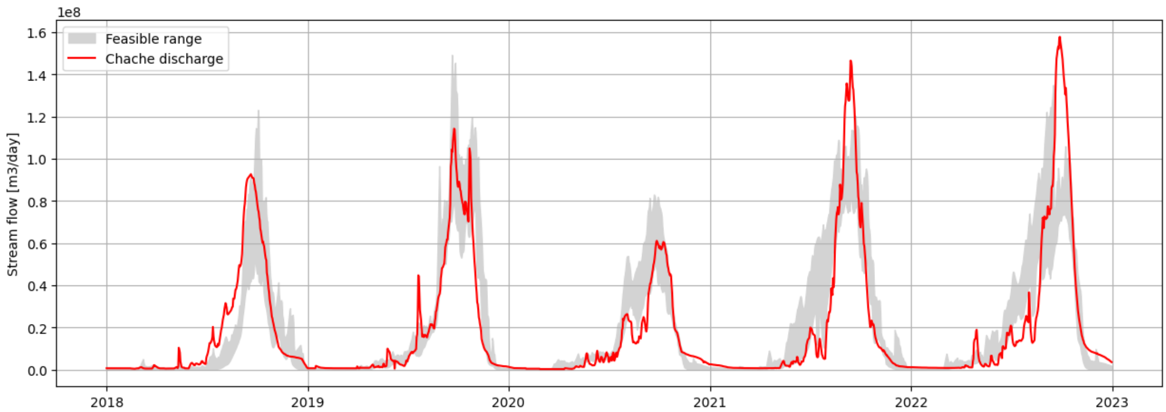

Figure 4.14: Testing the model with TAHMO precipitation, without further recalibration resulting in an NSE of 0.74

2019. The parameter set used in the model was the same as the one that yielded the highest NSE in the calibration process (see Figure 4.10).

The first model simulation using only TAHMO data was made on October 9th (see Figure 4.15.a). On that day, the overall model output closely resembles the measured discharge in terms of shape even though the peak is slightly underestimated. Later on, significant precipitation events occurred between October 10th and 12th, causing the model to predict a small peak (subfigure b). Again different precipitation events were observed for the dates 13th to 15th causing the model to predict a larger peak see Figure 4.15.c. From the 15th to the 19th, few precipitation events were recorded, and the discharge in Chache continued to decrease, while the model still predicted a significant peak. On the 21st, the last major precipitation event occurred, ultimately resulting in the measured peak in Chache on the 22nd and leading to the spill being utilized on the 23rd. In the last subfigure (f), the model over the year was compared to the cache discharge and it can be seen that both modeled peaks were underestimated compared to the actual measured values, but the proportion and shape were similar.

In conclusion, as early as October 12th, the model predicted the occurrence of a second peak, and by the 15th updated to grow larger, and on the 21st, it confirmed that the size of the peak would be similar to the first peak earlier in the season. The specific actions the BPA (Black Volta Basin Authority) could have taken based on this information are beyond the scope of this research. However, utilizing the model in combination with the near real-time data from TAHMO stations would have provided them with a 12-day lead time to make informed decisions and effectively manage the reservoir to accommodate the second peak.

Testing with Lawra

A different approach to evaluate the model is by changing the final testing location. This was done by shifting from Chache to Lawra, situated 208 km upstream. Lawra is essentially located at the junction of catchments 1, 2, and 3. Due to this change in location, it was necessary to recalibrate the model, particularly to update the lag times.

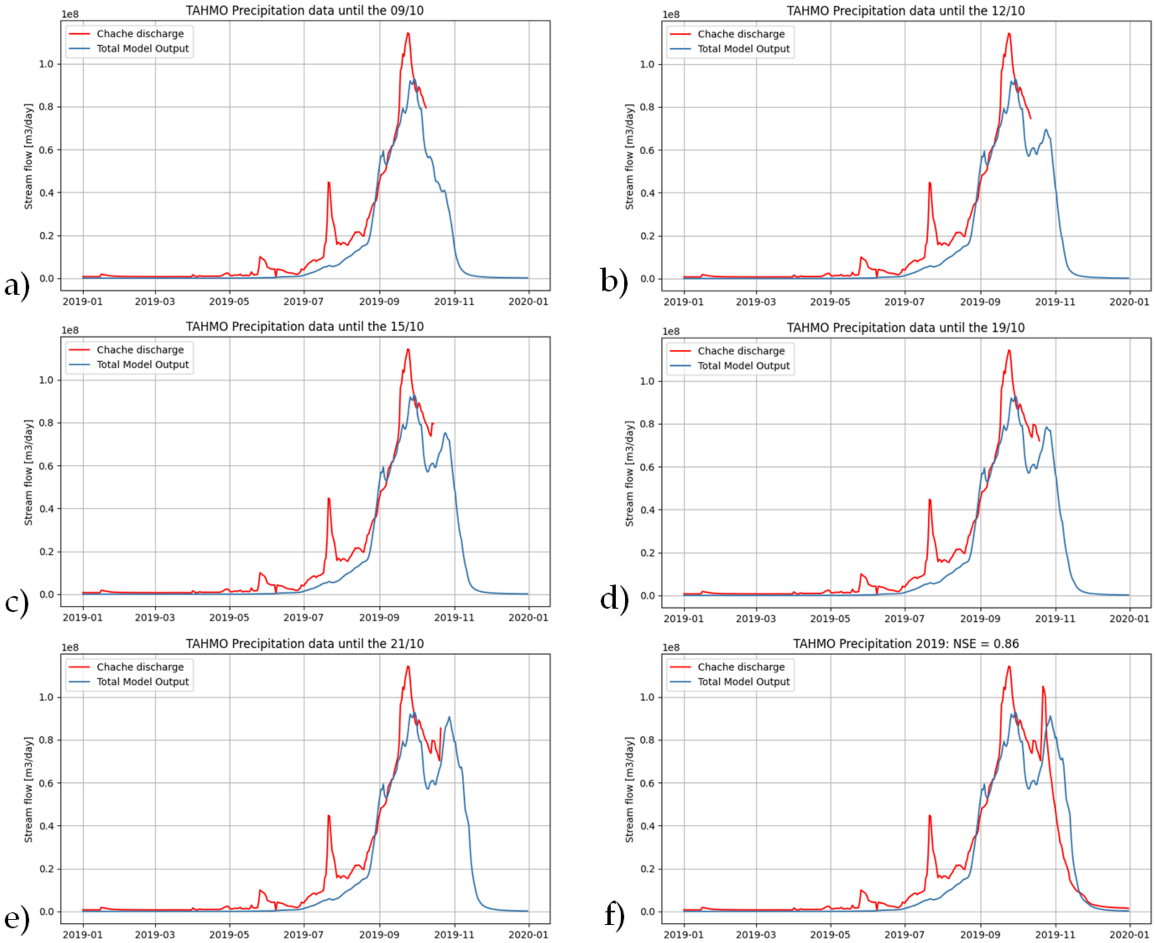

Figure 4.15: Model outputs updates based on TAHMO measured precipitation events. Going further in the month of October, the model predicts a higher peak

Following the construction of the dam, only four years of reliable and consistent data from BPA are available for analysis in Lawra.

To calibrate the Lawra discharge, it was decided to swap the years that were employed compared to the calibration of Chache. Specifically, the years 2013 to 2014 were used for Lawra calibration and 2020 and 2021 for testing, while Chache calibration utilized data from 2018 to 2022 calibration and 2013 to 2017 for testing (see Figure 4.13). The Lawra calibration process resulted in excellent results, with an NSE reaching up to 0.92, as illustrated in Figure 4.16.

The model was then tested without any further recalibration for the years 2020 and 2022, yielding NSE results of 0.79 and 0.84, respectively. The decrease in performance for the year 2020 can be attributed to the omission of modeling the initial smaller peak in August. Nevertheless, these results are satisfactory and are proving that the model is working well in different conditions.

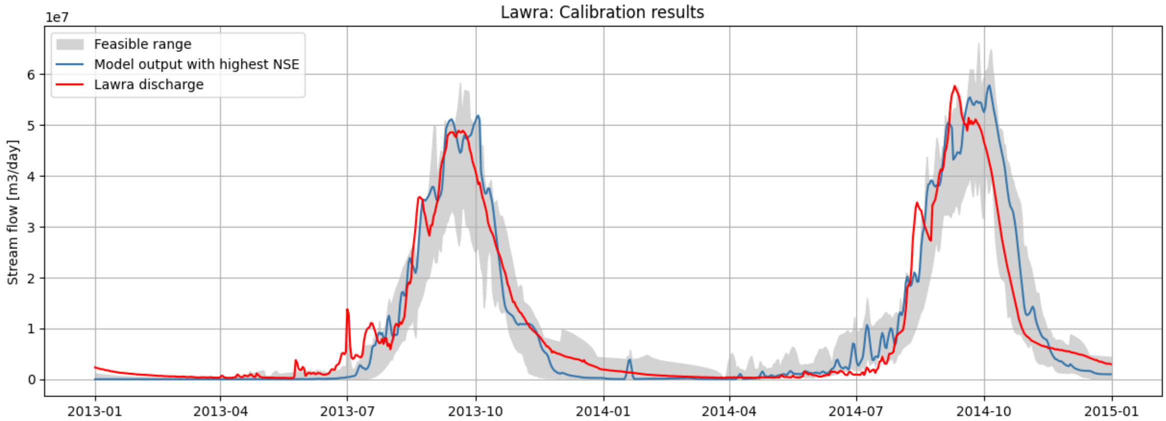

Figure 4.16: Calibration results for Lawra discharge, excellent NSE of 0.92

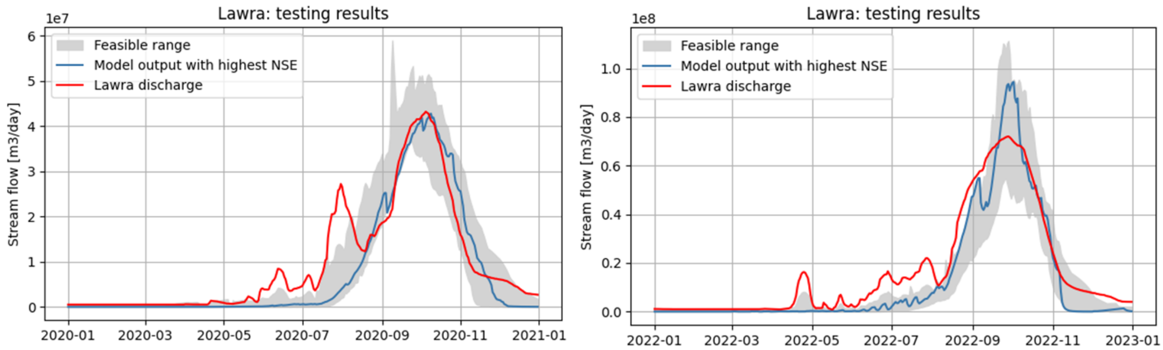

Figure 4.17: Testing results for Lawra discharge, independent time period without further recalibration. There is a drop in performance for the Figure on the left due to not modeling the first small peak

Testing with PET

For this last part, to address the limitation of the length of the AET dataset, modifications were made to the code to allow the switch from AET to PET. This modification allows for further testing of the model's performance under different conditions (before 2009 and thus before the construction of the dam). The alteration was implemented in equation 3.7, which involved the inclusion of two new parameters: C_e and m, and the following equation:

$$E_{act} = C_e * E_{pot} * \left(\frac{\bar{S} * (1 + m)}{\bar{S} + m} \right) \tag{4.3}$$

The parameter range for C_e is 0.46-0.90 and m is 0.2 to 1.5. Because of the change of code, the model was recalibrated and retested. To calibration used the years from 2003 to 2006 and the testing from 2006 to 2009. And resulted in an NSE of 0.85 and 0.83 respectively.

When analyzing Figure 4.18, it can be observed that the year 2003 had a similar "double peak" shape as the one in 2019, which was again well plotted by the model. However, it must be noted that the cumulative discharge in 2019 was about 35% bigger than the one in 2003.

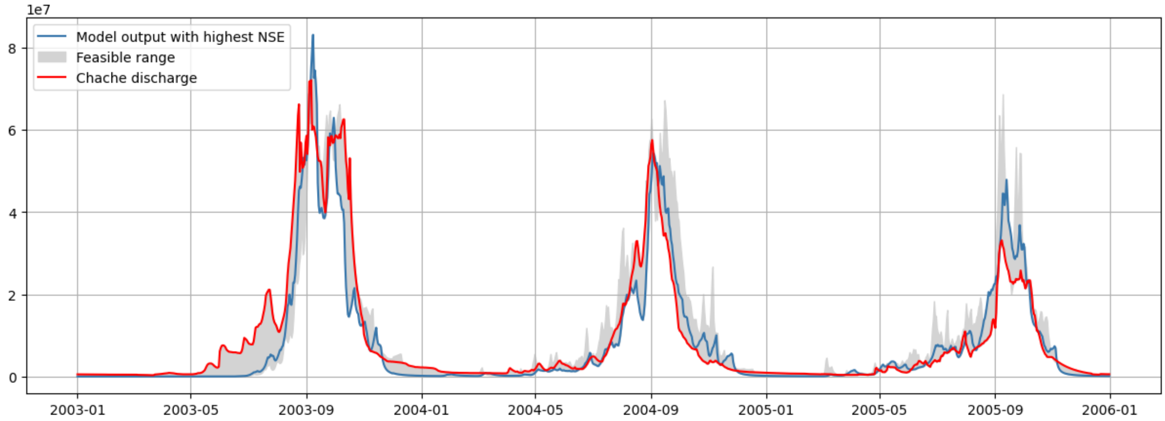

Figure 4.18: Calibration results for Chache discharge with PET

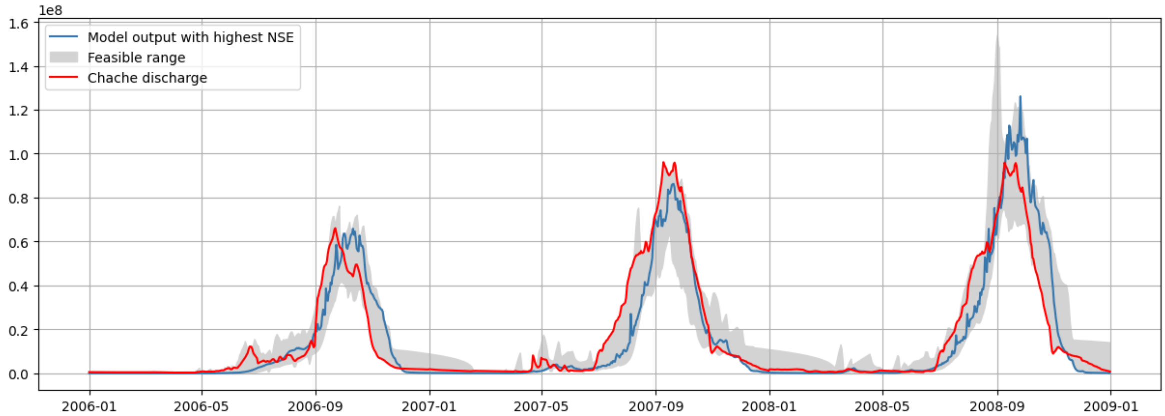

Figure 4.19: Testing results for Chache discharge with PET, independent time period without further recalibration NSE 0.83

4.2.5 Discussion

The challenge associated with developing hydrological models lies in establishing a quantitative relationship between the input, state, and output of the system. It is important to recognize that each model employed represents a hypothesis and, at best, offers an incomplete depiction of reality. Analytically solving this problem proves to be infeasible, necessitating numerical approaches. In the present study, as explained in Section 3.2.2, the numerical method known as Implicit Euler was employed. However, no investigations were conducted to explore alternative methods and compare their outcomes.

Furthermore, it is worth noting that numerous other calibration/evaluation methods exist, such as the Autocorrelation Function and Rising Limb Density, among others. In this report, only the Pareto optimal solution is utilized. The stochastic Monte-Carlo sampling method was employed to determine the best parameter set. This approach represents the ”purest” search strategy and relies on a brute-force method due to the extensive simulations required. Although time-consuming, this method provides a reasonable approximation of the parameter set. However, it should be acknowledged that discovering the absolute best parameter combination is highly unlikely. It is important to recognize that there are alternative stochastic and evolutionary strategies available that lie outside of the scope of this research.

The modeling approach employed in this study involved dividing the Black Volta Basin into five sub-catchments and subsequently aggregating them into a semi distributed model. Five distinct conceptual models were investigated, which can be categorized into three different structures: single (M1), serial (M2 & M3), and parallel (non-linear: M4 & HBV) structures. And ultimately, the M3 model was applied to each catchment because of its superior performance. However, it is essential to acknowledge that the models utilized in this research were relatively simplistic in their design and lumped many processes.

The threshold for determining the start and end of the Sourou extraction, a relatively rare occurrence characterized by a change in river discharge flow direction, was established based on monthly mean data spanning from 1956 to 1970. Later, in 1984, a regulation basin was constructed, which undoubtedly influenced the river's regulation. Also, working with monthly data from this time period is not ideal, it was the best available solution due to the scarcity of alternative data sources.

The spill that occurred in 2019 was primarily triggered by an unexpectedly wet October month, resulting in a second peak in the hydrograph. This peak was caused by three significant precipitation events. The hydrological model, using the parameter set that yielded the highest NSE during the calibration, successfully predicted the occurrence of the second peak 12 days in advance, but only provided a 5-day lead time regarding its magnitude. This limited time frame poses a real challenge for proactive reservoir management and reduces the opportunity to release water in preparation for such events.

Also, it is important to note that literally all the previous research conducted on hydrological modeling in the Black Volta Basin (Jung [2006], Akpoti et al. [2016], Sawai et al. [2014], Shaibu et al. [2012], Kwakye and Bárdossy [2020] and even the most recent Logah et al. [2023]) have calibrated and tested the model with discharge up until 2008. This is why comparing the results from these models is complicated since the construction of the Bui reservoir, completed in 2013, has had a substantial impact on the basin's hydrology. Notably, the discharges observed in the last five years have exhibited considerable differences when compared to pre-dam discharges. Therefore, it is important to recognize the limitations of previous research that did not account for these changes, as their findings may not fully reflect the current hydrological conditions and system behavior.

5 Conclusion

In the initial phase of this research, data collection was conducted in the Black Volta basin, encompassing daily precipitation and discharges recorded between 1991 and 2022. The collected data underwent a process of verification, aiming to ensure accuracy and consistency. Subsequently, necessary corrections were applied, culminating in the update of the rating curve in Chache. This update was done using a conservative approach of the reservoir water balance of the Bui reservoir. This part of the research answered the first sub-research question:*"Which datasets are available and reliable enough to be used to calibrate and test the hydrological model"*.

The basin was divided into five sub-catchments, each of which was assigned a conceptual model known as 'M3'. This model incorporated two reservoirs connected in series: one unsaturated reservoir and one fast reservoir linked through a lag function. The overall model output was then calibrated with the updated Chache discharge from 2018 to 2022, demonstrating favorable results when assessed on a daily time scale. The calibration process resulted in an NSE value of 0.85 (for 2018-2022). During the independent testing phase from 2013 to 2016, without further recalibration, the NSE value increased to 0.86. This higher testing result is uncommon in hydrological modeling. It can be attributed to the unusual rainfall-runoff distribution in 2019 and 2022, which made it more challenging to model and affected the calibration results. In contrast, the testing years from 2013 to 2016 showed a more typical rainfall-runoff pattern.

Moreover, the model underwent additional testing by employing a different discharge station situated in Lawra, approximately 208 km upstream of Chache. Because of the new setup, the model had a recalibration that resulted in a great NSE of 0.92 (for 2013-2014) and satisfactory testing results of 0.81 (for 2020 and 2022). Again proving the functioning of the hydrological model in the Black Volta Basin and answers the main research question: *"How can the daily discharge be effectively modeled in the data-scarce Black Volta Basin?"*

Incorporating TAHMO data from 2019 proved instrumental in anticipating the occurrence of an "unexpected" second peak on October 22nd to some extent, as early as October 12th. On that day the model predicted the occurrence of a second peak, which was updated to grow larger on the 15th, and on the 21st, it confirmed that the size of the peak would be similar to the first peak earlier in the season. By utilizing the model in conjunction with near real-time data from TAHMO stations, the Basin Power Authority (BPA) could have gained a 12-day lead time to make informed decisions and effectively manage the reservoir to accommodate the second peak. This answered the second sub-question: *"Could the spills of 2019 (and 2022) be avoided using a hydrological model and TAHMO precipitation inputs?"*

Most importantly, the basin modeling process provided valuable insights into the catchment characteristics that can be utilized for future research endeavors. One notable insight emerged from the Sourou extraction, which functions as a natural regulator of the Mouhoun River's discharge, revealing the limited impact of catchments 4 and 5 on peak flows in Chache or Lawra. Another significant observation was made during high-flow years, wherein catchment 2 exhibited a substantial impact compared to the other catchments and ultimately contributed significantly to the spill in 2019 an 2022. This answers the third sub-research question: *"What is the impact of the different sub-catchments on the total discharge of the Black Volta"*

Consequently, it is recommended to augment the hydrology information in catchment 2 to enhance informed decision-making in reservoir management. This could be achieved through the installation of a new discharge station or additional precipitation stations, thereby promoting a more comprehensive understanding of the catchment's dynamics.

6 Recommendations

As explained in the section 4.1.2 the rating curve was updated in a conservative approach. However, to further minimize the conservative approach and enhance the certainty and reliability of data for future modeling, it is advisable to update the Chache rating curve using a conventional and up-to-date measurement approach. This would involve conducting actual measurements to establish a more accurate relationship between water levels and discharge. The new rating curve, represented by Equation 4.2, can then serve as an upper bound for future research and analysis. By employing this approach, the accuracy and precision of the modeling outcomes can be significantly improved.

The decision to adopt a semi-distributed modeling approach instead of a gridded one was primarily driven by the limited availability of data in the region, particularly with regard to daily-scale precipitation. However, recent research conducted by Logah et al. [2023] demonstrated that by combining ground precipitation stations with satellite rainfall products, it is possible to develop a daily gridded hydrological model with high accuracy (NSE of 0.73-0.85). Updating to a gridded model by incorporating data from satellite products and TAHMO stations has the potential to yield an accurate and valuable decision-making tool for reservoir management.

But staying in the context of semi-distributed models, only five (divided in the function of their structure: single (M1), serial (M2 & M3), and parallel (non-linear: M4 & HBV)) were made and tested in this research. While the selected M3 model exhibited favorable performance, it is essential to recognize that the models tested in this research were relatively simplistic and may not capture the full complexity of the system. There is ample room for improvement and extension of these models. Future investigations can explore incorporating additional variables, refining model structures, and incorporating more advanced techniques to enhance the accuracy and reliability of the models. By pursuing these avenues, a more robust and sophisticated modeling framework can be established, enabling better insights and predictions in the study area.

For future research, it is recommended to strive for a higher level of certainty in modeling the impact of the Sourou extraction on the Black Volta Basin. This can be achieved by incorporating more recent and comprehensive data, particularly at finer temporal scales. Obtaining a more robust understanding of the dynamics associated with the Sourou extraction will enhance the accuracy and reliability of the modeling results.

The large magnitude of the second peak causing the spill in 2019 could only really be predicted with 5 day lead time using the TAHMO precipitation and the hydrological model. The limited lead time poses a real challenge for reservoir management. To overcome this it is recommended to explore the feasibility of incorporating weather forecasts into the hydrological model and the decision-making process, which could potentially extend the limited temporal window for preparation. Discussions with representatives from BPA have indicated that weather forecasts in Ghana, particularly in predicting significant rainfall events, tend to be reasonably accurate in terms of precipitation amounts. However, the accuracy in pinpointing the precise timing of precipitation events can be less reliable. Nonetheless, further investigation into the integration of weather forecasts into reservoir management practices is warranted. Assessing the accuracy of the previous year's weather forecasts and comparing them with actual precipitation data would be essential in evaluating the viability of this approach.

The model calibration process involved, in part, the utilization of satellite altimetry data and the calculation of the relative error between water level observations and modeled discharge. However, this approach assumes a monotonous relationship between the two variables, which is a significant assumption to make. Therefore, it is advisable to consider incorporating river geometry and friction to convert modeled discharge into water levels, as suggested by Hulsman et al. [2020]. Regrettably, due to time constraints in this research, this step was not undertaken, but it is strongly recommended for future investigations.

Another aspect that warrants further research is the integration of soil moisture satellite data into the model. This type of data can be highly valuable in determining soil saturation levels and, consequently, in providing insights into reservoir saturation within the model. Previous studies have indicated that the saturation point can undergo significant shifts in the Volta region within a matter of days and this is closely related to a sudden increase in the discharge. Therefore, if a soil moisture satellite product is to be implemented, it is recommended to adopt a daily temporal resolution. The RZSM-ASCAT-NRT-10 (H26) product from EUMETSAT, which has been available since 2022, appears to be the most suitable choice for future research endeavors.

Bibliography

Akpoti, K., Antwi, E. O., and Kabo-bah, A. T. (2016). Impacts of rainfall variability, land use and land cover change on stream flow of the black volta basin, west africa. *Hydrology*, 3(3):26.

Andreini, M., Giesen, N., Edig, A., Fosu, M., and Andah, W. (2000). Volta basin water balance. Technical report, ZEF discussion papers on development policy.

Bastiaanssen, W., Cheema, M., Immerzeel, W., Miltenburg, I., and Pelgrum, H. (2012). Surface energy balance and actual evapotranspiration of the transboundary indus basin estimated from satellite measurements and the etlook model. *Water Resources Research*, 48(11).

Beven, K. (1989). Changing ideas in hydrology—the case of physically-based models. *Journal of hydrology*, 105(1-2):157–172.

Block, P. (2011). Tailoring seasonal climate forecasts for hydropower operations. *Hydrology and Earth System Sciences*, 15(4):1355–1368.

Bro, C. (2001). Etat des lieux des ressources en eau du burkina faso et de leur cadre de gestion. Ministere de l'environnement et de l'eau, Burkina Faso.

Centre, G. R. D. (2019). The global runoff data centre, 56068 koblenz, germany.

Consult, A. (2012). Diagnostic study of the black volta basin in ghana. *Final Report*.

Dal Molin, M., Kavetski, D., and Fenicia, F. (2021). Superflexpy 1.3. 0: an open-source python framework for building, testing, and improving conceptual hydrological models. *Geoscientific Model Development*, 14(11):7047–7072.

Dembélé, M. and Zwart, S. J. (2016). Evaluation and comparison of satellite-based rainfall products in burkina faso, west africa. *International Journal of Remote Sensing*, 37(17):3995–4014.

Dowell, M. and Jarratt, P. (1972). The "pegasus" method for computing the root of an equation. *BIT Numerical Mathematics*, 12:503–508.

FAO (1998). World reference base for soil resources world soil resources report 84. Technical report, Food and Agriculture Organization of the United Nations, Rome.

FAO (2018). WaPOR Database Methodology: Level 1. Remote Sensing for Water Productivity Technical Report: Methodology Series. Technical report, Rome, FAO. Licence: CC BY-NC-SA 3.0 IGO.

Farr, T. G., Rosen, P. A., Caro, E., Crippen, R., Duren, R., Hensley, S., Kobrick, M., Paller, M., Rodriguez, E., Roth, L., et al. (2007). The shuttle radar topography mission. *Reviews of geophysics*, 45(2).

Fenicia, F., Kavetski, D., and Savenije, H. H. (2011). Elements of a flexible approach for conceptual hydrological modeling: 1. motivation and theoretical development. *Water Resources Research*, 47(11).

Funk, C., Peterson, P., Landsfeld, M., Pedreros, D., Verdin, J., Rowland, J., Romero, B., Husak, G., Michaelsen, J., and Verdin, A. (2014). A quasi-global precipitation time series for drought monitoring. Technical Report 832, U.S. Geological Survey.

Hamlet, A. F., Huppert, D., and Lettenmaier, D. P. (2002). Economic value of long-lead streamflow forecasts for columbia river hydropower. *Journal of Water Resources Planning and Management*, 128(2):91–101.

Hrachowitz, M. and Clark, M. P. (2017). Hess opinions: The complementary merits of competing modelling philosophies in hydrology. *Hydrology and Earth System Sciences*, 21(8):3953–3973.

Hrachowitz, M., Fovet, O., Ruiz, L., Euser, T., Gharari, S., Nijzink, R., Freer, J., Savenije, H., and Gascuel-Odoux, C. (2014). Process consistency in models: The importance of system signatures, expert knowledge, and process complexity. *Water resources research*, 50(9):7445–7469.

Hulsman, P., Winsemius, H. C., Michailovsky, C. I., Savenije, H. H., and Hrachowitz, M. (2020). Using altimetry observations combined with grace to select parameter sets of a hydrological model in a data-scarce region. *Hydrology and Earth System Sciences*, 24(6):3331–3359.

Jin, L., Whitehead, P. G., Addo, K. A., Amisigo, B., Macadam, I., Janes, T., Crossman, J., Nicholls, R. J., McCartney, M., and Rodda, H. J. (2018). Modeling future flows of the volta river system: Impacts of climate change and socio-economic changes. *Science of the Total Environment*, 637:1069–1080.

Jung, G. (2006). Regional climate change and the impact on hydrology in the volta basin of west africa.

Kirchner, J. W. (2009). Catchments as simple dynamical systems: Catchment characterization, rainfall-runoff modeling, and doing hydrology backward. *Water Resources Research*, 45(2).

Kwakye, S. O. and Bárdossy, A. (2020). Hydrological modelling in data-scarce catchments: Black volta basin in west africa. *SN Applied Sciences*, 2(4):628.

Landerer, F. W. and Swenson, S. (2012). Accuracy of scaled grace terrestrial water storage estimates. *Water resources research*, 48(4).

Lima, C. H. and Lall, U. (2010). Climate informed monthly streamflow forecasts for the brazilian hydropower network using a periodic ridge regression model. *Journal of hydrology*, 380(3-4):438–449.

Logah, F. Y., Adjei, K. A., Obuobie, E., Gyamfi, C., and Odai, S. N. (2021). Evaluation and comparison of satellite rainfall products in the black volta basin. *Environmental Processes*, 8:119–137.

Logah, F. Y., Obuobie, E., Adjei, K. A., Gyamfi, C., and Odai, S. N. (2023). Capability of satellite rainfall products in simulating streamflows in the black volta basin. *Sustainable Water Resources Management*, 9(3):1–14.

Menne, M. J., Durre, I., Korzeniewski, B., McNeal, S., Thomas, K., Yin, X., Anthony, S., Ray, R., Vose, R. S., Gleason, B. E., et al. (2012). Global historical climatology network-daily (ghcn-daily), version 3. *NOAA National Climatic Data Center*, 10:V5D21VHZ.

Mu, Q., Zhao, M., and Running, S. W. (2011). Improvements to a modis global terrestrial evapotranspiration algorithm. *Remote sensing of environment*, 115(8):1781–1800.

Nash, J. E. and Sutcliffe, J. V. (1970). River flow forecasting through conceptual models part i—a discussion of principles. *Journal of hydrology*, 10(3):282–290.

Obeng-Asiedu, P. (2004). Allocating water resources for agricultural and economic development in the volta river basin.

Ries, J., Bettadpur, S., Eanes, R., Kang, Z., Ko, U.-d., McCullough, C., Nagel, P., Pie, N., Poole, S., Richter, T., et al. (2016). The development and evaluation of the global gravity model ggm05. Technical report.

Satgé, F., Defrance, D., Sultan, B., Bonnet, M.-P., Seyler, F., Rouché, N., Pierron, F., and Paturel, J.-E. (2020). Evaluation of 23 gridded precipitation datasets across west africa. *Journal of Hydrology*, 581:124412.

Savenije, H. H. (2001). Equifinality, a blessing in disguise? *Hydrological processes*, 15(14):2835–2838.

Sawai, N., Kobayashi, K., Takara, K., Ishikawa, H., Yokomatsu, M., Samaddar, S., Juati, A.-N., Kranjac-Berisavljevic, G., et al. (2014). Impact of climate change on river flows in the black volta river. *Journal of Disaster Research*, 9(4):432–442.

Schwatke, C., Dettmering, D., Bosch, W., and Seitz, F. (2015). Dahiti–an innovative approach for estimating water level time series over inland waters using multi-mission satellite altimetry. *Hydrology and Earth System Sciences*, 19(10):4345–4364.

Searcy, J. K. and Hardison, C. H. (1960). *Double-mass curves*. Number 1541. US Government Printing Office.

Seibert, J. and Vis, M. J. (2016). How informative are stream level observations in different geographic regions? *Hydrological Processes*, 30(14):2498–2508.

Shahin, M. (2003). *Hydrology and water resources of Africa*, volume 41. Springer Science & Business Media.

Shaibu, S., Odai, S. N., Adjei, K. A., Osei, E. M., and Annor, F. O. (2012). Simulation of runoff for the black volta basin using satellite observation data. *International journal of river basin management*, 10(3):245–254.

Shoemaker, W. B. and Sumner, D. M. (2006). Alternate corrections for estimating actual wetland evapotranspiration from potential evapotranspiration. *Wetlands*, 26(2):528–543.

Strahler, A. N. (1957). Quantitative analysis of watershed geomorphology. *Eos, Transactions American Geophysical Union*, 38(6):913–920.

Thiessen, A. H. (1911). Precipitation averages for large areas. *Monthly weather review*, 39(7):1082–1089.

Weerasinghe, I., Bastiaanssen, W., Mul, M., Jia, L., and van Griensven, A. (2020). Can we trust remote sensing evapotranspiration products over africa? *Hydrology and Earth System Sciences*, 24(3):1565–1586.